COMMONWEALTH OF AUSTRALIA

BUREAU OF METEOROLOGY

DEPARTMENT OF THE INTERIOR

WSM

Working Paper No. 119
65/7 of August 1969

SOLAR INFRARED RADIATION IN THE ATMOSPHERE

Review lecture delivered to the Symposium on Atmospheric Physics, 41ST ANZAAS Congress, Adelaide, August 1969

by

J.W. Zillman
Central Office, Bureau of Meteorology,
Melbourne.

SR Rcd 15/4/71
SSM
WSM

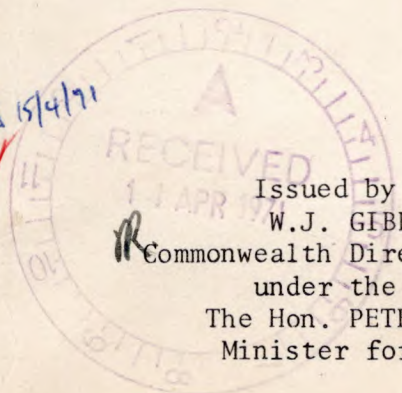

Issued by direction of
W.J. GIBBS, O.B.E.
Commonwealth Director of Meteorology
under the authority of
The Hon. PETER NIXON, M.P.
Minister for the Interior

The "Working Paper" series of publications is designed as a means of circulating to fellow scientists, both within and outside the Bureau, the progress achieved on a problem of meteorological interest when a major phase in the investigation has been completed. This publication is generally not an end product but rather a preliminary stage in the preparation of a scientific paper for publication.

Meteorological "Working Papers" are intended for both internal and external distribution. The external distribution will depend on the content of the particular Working Paper.

Reference to the paper should be made in the following manner:

"Bureau of Meteorology Working Paper No. 119
65/7 of August 1969"

CONTENTS

		Page
Abstract		1
Introduction		1
The Sun's Thermal Radiation		3
Solar Radiation in the Atmosphere		6
The Response of the Atmosphere		21
References		29
Appendix I	Symbols and Nomenclature	3 pages
Appendix II	Bibliography	4 pages

Working Paper 65/7 of August 1969

SOLAR INFRARED RADIATION IN THE ATMOSPHERE

by

J.W. Zillman

Central Office, Bureau of Meteorology, Melbourne

ABSTRACT

This review treats briefly the part played by infrared solar radiation in determining the thermal and dynamic structure of the earth's atmosphere. It begins with the solar source of thermal radiation and its amount and spectral composition at the outer limits of the atmosphere. The essential aspects of the interaction between the solar beam and the atmospheric constituent gases, aerosols and clouds follow from a simple formulation of the radiative transfer equation and lead to estimates of the spectral and integral solar beam transmission by the atmosphere, its absorption-heating and the energy input to its lower boundary. From this, attention turns to the response of the earth-atmosphere system to the imposed power input; in particular the part played by low-temperature thermal radiation in countering continued energy localisation and storage over particular parts of the planet's surface and through the depths of its atmosphere; the absence of radiative equilibrium in the atmosphere and the necessity for energy transport by the oceans and atmosphere to counter the radiation imbalance; and finally to a picture of the atmospheric circulation as an exceedingly inefficient heat engine maintained against the dissipative forces of friction by a small part of the continuous solar power input.

1. INTRODUCTION

The thermal radiation emanating from the sun constitutes the ultimate energy source for almost all physical and biological processes on the planet: it maintains our atmosphere at a temperature which will sustain life; it provides the power necessary to maintain the kinetic energy of winds and seas against continuous dissipatation by friction; it provides the tremendous reserves of fuel we burn and food we eat and the water resources which we harness for domestic power and industry. The sequence of physical processes involved constitutes a

problem of fascinating complexity. The most obvious immediate effect of solar radiation on our environment is absorption-heating but the thermal energy realised is distributed unequally over the earth and through the depths of its atmosphere. It is almost three centuries since Halley (1686) attributed to this the existence of the monsoons and trade wind systems of the tropical oceans and so laid the foundations of a still incomplete theory. Experimental and theoretical study of the storage, conversion and redistribution of absorbed solar radiant energy by dynamical and radiative processes and its ultimate return to space as low-temperature thermal radiation remains one of the central themes in meteorology.

The great problem in the study of the atmosphere arises from the non-linearity and complexity of the governing equations. Ideally, granted that the sun is the only external energy source all the physical properties of the atmosphere should be predictable for any future time given only the governing equations, initial state and imposed boundary condition of a certain (time-dependent) solar radiation flux. Realisation of this ideal is still far off and our understanding even of the basic physics of the interaction between solar radiation and the terrestrial atmosphere is still far from complete. However, we can gain considerable insight into the behaviour of the atmosphere by examining relatively simple and largely qualitative answers to the following questions:

(i) How much energy is radiated by the sun, what fraction reaches the outer limits of the earth, how does it vary and what is its spectral composition?

(ii) What happens to it in the atmosphere, what does it do to the atmosphere, how much reaches the earth's surface and what effect has it there?

(iii) Why doesn't the planet get hotter; why aren't the poles colder? Is the atmosphere in radiative equilibrium; if not how is its thermal structure maintained and how is its circulation maintained?

The following sections present in turn some general answers to these questions and provide a selection of numerical values when these throw significant light on the discussion.

The elementary physics of radiation absorption and emission by solid and gaseous media is assumed but some of the problems peculiar to these processes under atmospheric conditions are mentioned briefly. Frequency or wavelength notation is used according to convenience and wavelength terminology is as illustrated in Fig. 3. Only thermal radiation is considered in this review and we are concerned primarily with the so-called shortwave ($\lambda<4\mu$) spectral range. The ultraviolet ($\lambda<0.38\mu$) part of the solar spectrum is not discussed explicitly being the topic of the companion review (Carver) but is accounted for in total power estimates for the solar beam. It is of interest that all energetically significant terrestrial (longwave, 4-50μ) radiation falls also within the infrared range.

The diverse systems of symbols and nomenclature to be found in the atmospheric radiation literature lend considerable confusion to the subject. Differing names and symbols, each hallowed by usage, are frequently applied to the same quantity and different quantities are to be found with the same name. The two main influences in the nomenclature employed here are the body of radiative transfer theory as formulated by Chandrasekhar (1950) and adapted from an astrophysical to an atmospheric emphasis by Goody (1964) and the recommendations of the Commission for Symbols, Units and Nomenclature of the International Union of Pure and Applied Physics (Wolfe, 1962). Because precise definition of terms and symbols is essential those introduced in the text without or with only vague definition are collected and defined in Appendix I. Text references have been kept to a minimum but a bibliography provided as Appendix II is intended as an introductory guide to the more recent basic literature.

2. THE SUN'S THERMAL RADIATION

2.1 The solar emission

The sun's energy derives from thermonuclear conversion of 4.2 million tons of matter every second deep within its ten million ^{o}K interior. Convective and radiative processes transport energy outwards to the region of the photosphere, the sharply-defined apparent solar surface of

radius 6.96 x 10^5 km. Energy streams out from the photosphere as thermal and non-thermal electromagnetic radiation and corpuscular radiation. The total power output, approximately 3.88 x 10^{26} watts, is almost exclusively as thermal radiation in the wavelength range 0.2 to 5.0μ and corresponds with the total thermal emission from a black body the size of the photosphere at a temperature of 5790°K. The spectral distribution however, is non-Planckian and in the near ultra-violet, visible and near infrared is nearer to black body emission at 6000°K. It consists of a continuous emission due to unquantised electronic transitions and a superposed line spectrum (the Fraunhofer spectrum) apparent mostly as absorption lines, but of energetic significance only in the ultraviolet.

2.2 *The radiation reaching the outer limits of the earth's atmosphere, its magnitude, variation and spectral composition*

The earth moves on a very slightly elliptical orbit around the sun, distant 147.1 million kilometres at perihelion and 152.1 million kilometres at aphelion. At "mean solar distance" (149.6 x 10^6 km) when the sun subtends approximately 32.0 minutes of arc the solar irradiance (energy per unit time through unit area normal to the radius vector) referred to as the "solar constant" has a value within 2% of 1380 watts metre^{-2} (1.98 cal cm^{-2} min^{-1}) Ignoring for the present reflection from the earth and its atmosphere we can compute the corresponding solar radiant power intercepted by the whole earth. It is 1.76 x 10^{17} watts, quite small if one considers that at this rate it takes us 4200 years to intercept the solar output of a single minute; yet by comparison with more familiar terrestrial phenomena it is very great indeed. For example the solar power intercepted by the planet is equivalent to:

(i) seven hundred million times the electrical power consumption of a city like Adelaide;

(ii) one hundred million Hiroshima bombs per day;

(iii) that necessary to bring the circulation of the atmosphere to a standstill within an hour and a quarter;

or (iv) to melt all the ice of Antarctica in 15 months.

The elliptic orbit of the earth results in an approximately 3½% variation in the extra-terrestrial radiation either side of the solar constant with greatest values during the southern hemisphere summer. Apart from this the question of possible variation of the solar constant arises. Geological and paleontological evidence indicates that the sun has radiated at about its present rate for at least a billion years though cyclic variations in the eccentricity of the earth's orbit with a period of some 92,000 years (Lamb, 1966) imply an annual range in extra-terrestrial radiance as great as 30% in the past and distant future. On time scales from minutes to years despite large variations in the ultraviolet and x-ray emission and million-fold fluctuations at radio (metre) wavelengths the total (i.e. wavelength integrated) power output appears to remain essentially constant. Variation of total emission with Zurich sunspot number has been suggested, but on presently available evidence, is not established. Long-period correlation between weather elements and the sunspot cycle and other solar transients as suggested by lake levels, glacier retreat, growth rings and so forth may be due to some triggering effect resulting from variation in ultra-violet absorption high in the atmosphere but the mechanism of downward propagation is not clear.

Whilst the total, i.e. wavelength integrated, power per unit area normal to the solar beam beyond the atmosphere varies by only a few percent the power *per unit area of the earth's surface* (in the absence of an atmosphere) varies markedly through the day and with latitude and season being proportional to the sine of the elevation of the sun above the horizon. The *daily average* value is a function only of latitude (ϕ) and season (solar declination δ) and for a solar constant of 1380 watts metre^{-2} (1.98 cal cm^{-2} min^{-1}) is given in watts metre^{-2} by:

$$S_{VE} = \frac{1380}{\pi} \left(\frac{\bar{r}}{r}\right)^2 (H \sin \phi \sin \delta + \cos \phi \cos \delta \sin H) \quad \ldots(1)$$

Its variation with latitude and time of year is shown in Fig. 1 for southern latitudes. Frequently monthly average values of the undepleted insolation S_{VE} are required. These are shown as a function of latitude in Fig. 2 based on recent computer summations (Kubota, 1967).

Fig. 3(a) compares the solar spectral irradiance normal to the solar beam beyond the atmosphere with that from a 6000°K black body photosphere at mean sun-earth distance. It is seen that the solar spectral irradiance cannot be characterised by any single black body temperature distribution. Slightly more than 99% of the total energy falls within the so-called shortwave range ($\lambda<4.0\mu$); of this 48% is within the infrared ($\lambda>0.72\mu$) and 44% in the visible region of the solar spectrum (0.38 -0.72μ).

3. SOLAR RADIATION IN THE ATMOSPHERE

3.1 Radiative transfer in the earth's atmosphere

Because it involves a large number of selectively absorbing, scattering and emitting constituents, non-uniformly distributed in space and variable with time the general problem of thermal radiative transfer in the terrestrial atmosphere is extremely complicated.

Formally it is described by the equation of radiative transfer

$$\frac{\partial I_\nu}{\partial r} = k_\nu \rho \, (S_\nu - I_\nu) \qquad \ldots(2)$$

which in integral form for a beam directed from point O to point P along an optical path

$$U_p \quad (= \int_0^P k_\nu \rho \, dr) \quad \text{viz}$$

$$I_{\nu P} = I_{\nu o} \, e^{-U_p} + \int_0^{U_p} S_\nu \, e^{-U} \, dU \qquad \ldots(3)$$

shows that the intensity of radiation emerging from a certain layer of the atmosphere consists of two components: that incident on the layer attenuated in transit and that arising from within the atmospheric layer itself. Extinction may be due to any or all of absorption, scattering and reflection. The source function S_ν may correspond to thermal (in the lower atmosphere, Planckian) emission and/or scattering.

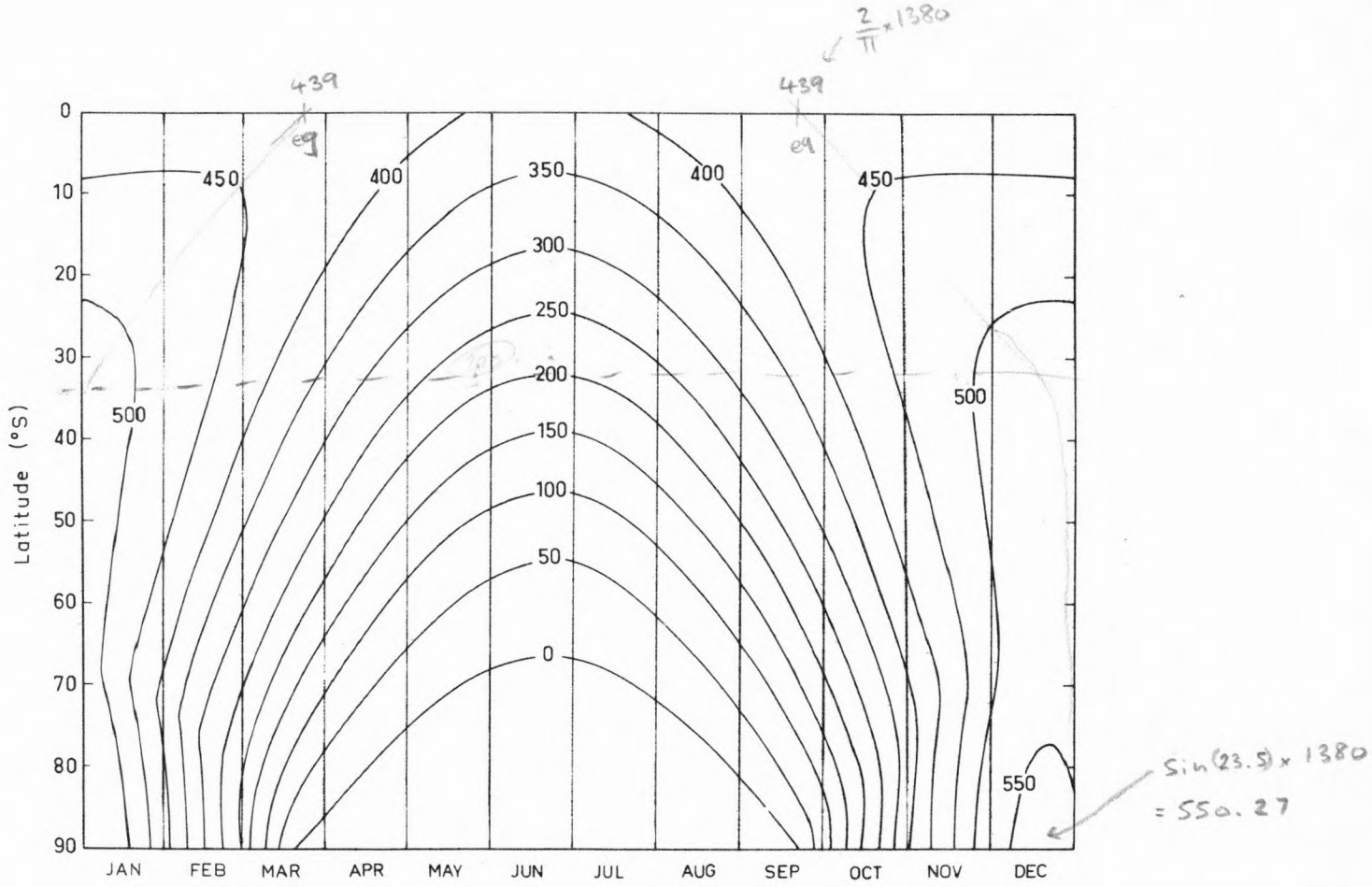

Figure 1. Daily average solar radiant power per unit area incident on the earth's surface in the absence of an atmosphere (undepleted insolation) as a function of latitude (°S) and time of year. Vertical markers correspond to the first day of each month and isopleths are labelled in watts metre^{-2}.

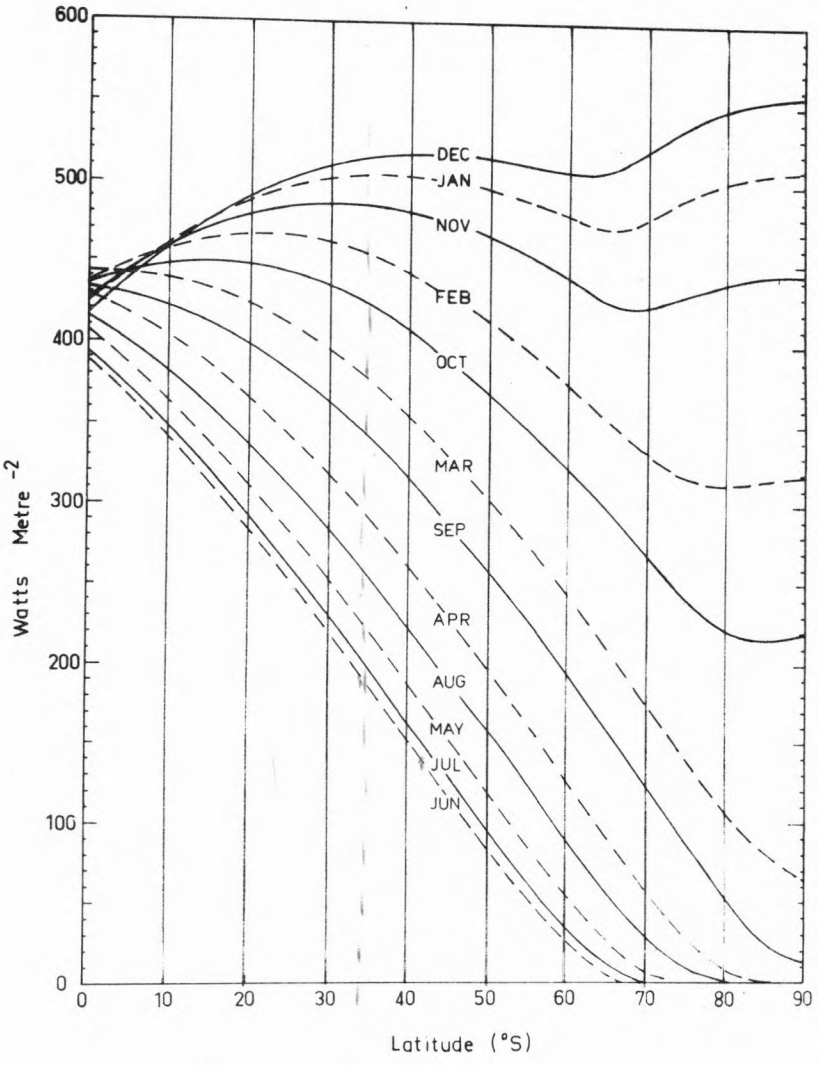

Figure 2. Monthly average undepleted insolation (watts metre $^{-2}$) as a function of latitude ($^{\circ}$S) compiled from Kubota (1967).

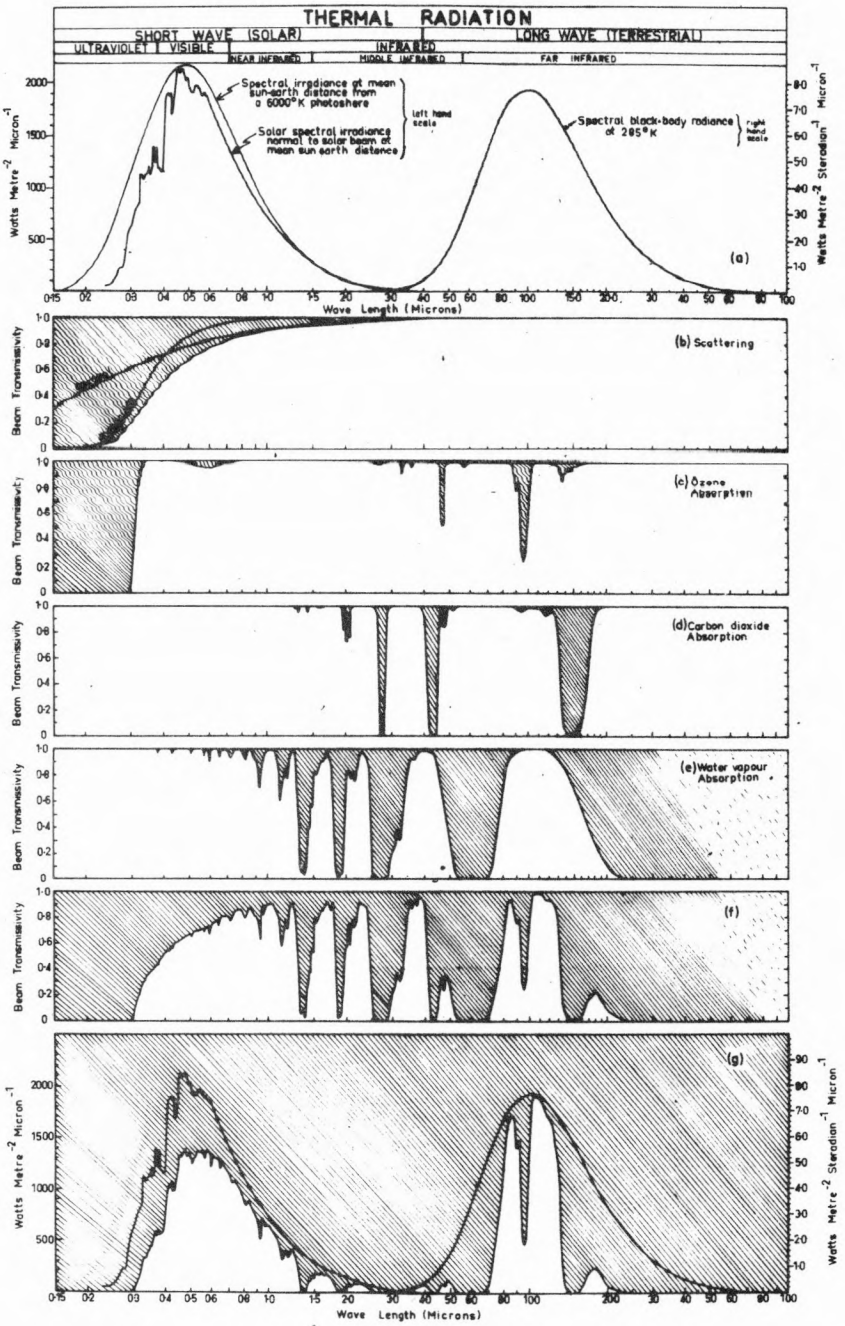

Figure 3. The thermal radiation spectrum:

(a) extraterrestrial solar spectrum compared with that of a 6000°K black body photosphere and black body emission at terrestrial temperatures.

(b) molecular and aerosol scattering transmissivities for a vertically incident beam with surface pressure 1000 millibars, Angström turbidity coefficient $\beta = 0.1$ and wavelength exponent $\alpha = 1.3$.

(c)–(e) vertical beam transmissivities for pressure scaled depths of 0.3 cm (NTP) of ozone, 100 cm (NTP) of carbon dioxide and one centimetre of precipitable water.

(f) vertical beam transmissivity resulting from a combination of (b) – (e).

(g) solar spectrum at sea level and the spectrum of vertically directed ground emission beyond the atmosphere from a combination of (a) and (f).

Equation (3) simplifies considerably if the source function can be neglected. For the solar (shortwave) radiation this is almost invariably assumed; thermal emission because it is very small at wavelengths for which the solar beam irradiance is large: scattering because it is too difficult to handle though its neglect may incur significant error except at wavelengths for which strong absorption occurs high in the atmosphere.

With the source function neglected and introducing as a shorthand notation the transmissivity $Q = e^{-\int k\rho \, dr}$ and zenith beam transmissivity $q = e^{-\int k\rho \, dz}$

$$I_\nu = I_{\nu 0} \, Q_\nu \qquad \ldots(4.1)$$

$$= I_{\nu 0} \, q_\nu^{m_r} \qquad \ldots(4.2)$$

where the relative optical path m_r is defined as the slant to zenith optical path ratio $\int k\rho \, dr / \int k\rho \, dz$.

The quantities Q_ν and q_ν are monochromatic *beam* transmissivities and describe the fraction of an incident beam which is transmitted through the layer from the outer limits of the atmosphere to the specified level (usually the surface) along slant and vertical paths respectively. They may represent the effect of one or several depleting media and processes and combine multiplicatively.

3.2 Spectral depletion by atmospheric constituents

Consider the solar beam with its spectral composition as in Fig. 3(a) penetrating the earth's atmosphere. The main depletion in a cloudless atmosphere will result from

(a)	Scattering by	(i)	air molecules
		(ii)	aerosol (dust, water vapour, haze)
(b)	Absorption by	(i)	ozone
		(ii)	carbon dioxide
		(iii)	water vapour

In general the depletion will vary markedly with wavelength particularly the absorption which occurs in discrete lines and bands. The three major absorbers listed together comprise no more than one percent by volume of the atmosphere. Such other minor constituents as the oxides of nitrogen and certain hydrocarbons contribute a few weak absorption bands and aerosol absorption occurs but is small also. Molecular oxygen plays a minor part in the low atmosphere and above 30 km there is a contribution from atomic oxygen. For a cloudy atmosphere the problem is immensely complicated by the absorption, scattering and reflection by clouds of variable shape and structure.

The monochromatic solar beam transmissivity for a cloudless atmosphere containing ozone, carbon dioxide and water vapour may be determined from an expansion of Equation 4 if the transmissivities for each constituent and process acting alone can be determined.

i.e.

$$Q_\nu = Q_{\nu sA}\ Q_{\nu sD}\ Q_{\nu a(O_3)}\ Q_{\nu a(CO_2)}\ Q_{\nu a(H_2O)} \qquad \ldots(5.1)$$

$$= \left(q_{\nu sA}\ q_{\nu sD}\ q_{\nu a(O_3)}\ q_{\nu a(CO_2)}\ q_{\nu a(H_2O)}\right)^{m_r} \qquad \ldots(5.2)$$

$$= (q_{\nu sA})^{m_r} T_\nu \qquad \ldots(5.3)$$

Equation 5.3 defines the Linke spectral turbidity factor T_ν which is a measure of the depletion by all processes except molecular scattering and may be taken as indicating the number of atmospheres of pure air which would attenuate the solar beam by the same factor. Equation 5.2 is in fact only an approximation because the relative optical path m_r is not quite the same for each attenuating constituent.

Values for the Q_ν and q_ν components of the right hand side of Equations 5.1 and 5.2 are derived in terms of the optical path length and optical depth of the atmosphere;

$$Q_{\nu i} = \exp\left(-\int \rho_i \, k_{\nu i} \, dr\right)$$

$$= \exp\left(-m_{ri} \int \rho_i k_{\nu i} dz\right)$$

$$q_{\nu i} = \exp\left(-\int \rho_i \, k_{\nu i} \, dz\right)$$

where the quantities normally available are:

(i) laboratory values of, or theoretical/empirical models for, the mass extinction coefficients $k_{\nu i}$ together with the form of their variation with ambient pressure, temperature, etc.

(ii) the integrated mass in the direction of the sun ($\int \rho_i \, dr$) or vertically ($\int \rho_i \, dz$) together with information on its distribution with respect to temperature and pressure.

Two scattering and three absorption transmissivities are considered briefly in turn below and illustrated for the case of zenith sun depleted by an atmosphere extending to sea level at 1000 mb and containing representative amounts of aerosol, ozone, carbon dioxide and water vapour.

3.3 Scattering depletion of the solar beam

(i) Molecular (Rayleigh) scattering.

The mass extinction coefficient due to scattering by the molecules of a pure dry atmosphere may be shown to take the form

$$k_{sA} = \frac{1}{f} \frac{32 \, H\pi^3 \, (n_\lambda - 1)^2}{3N \, \lambda^4} \qquad \ldots(6.1)$$

This leads to an expression for the transmissivity

$$Q_{\nu sA} = \exp(-m \; 0.00897 \; \lambda^{-4.09}) \qquad \ldots(6.2)$$

for a solar beam penetrating to sea level. Its value for zenith sun is shown in Fig. 3(b). It is seen that a pure Rayleigh atmosphere is almost opaque at $\lambda = 0.2\mu$ but, for zenith sun, almost completely transparent at $\lambda > 1.0\mu$.

(ii) Aerosol scattering

The theory of scattering by dielectric spheres of radius $0.1\lambda<r<25\lambda$ is considerably more complex than that for Rayleigh scattering ($r\lesssim 0.1\mu$) and has not yet been satisfactorily adapted to treat solar beam depletion by atmospheric aerosol. Empirically aerosol extinction has been found to be wavelength dependent, though less so than for molecular scattering by an amount that depends on particle size. The corresponding transmissivity may be represented

$$Q_{\nu sD} = \exp\left(-m_r \beta \lambda^{-\alpha}\right) \qquad \ldots(7)$$

β being a measure of the aerosol content above the reference level known as the Angström turbidity coefficient. α is a parameter related to the aerosol particle size distribution and is frequently taken as 1.3. Adopting this value and an Angström turbidity coefficient of 0.100 (Darwin, Northern Australia in spring) the zenith sun transmissivity is as shown in Fig. 3(b). The overall transmissivity after scattering

$$Q_{\nu sA}\, Q_{\nu sD} = e^{-(m\ 0.00897\lambda^{-4.09} + m_r \beta \lambda^{-1.3})} \qquad \ldots(8)$$

is shown also for zenith sun.

3.4 Solar beam absorption

The visible and near infrared absorption is due to vibrational-rotational transitions of the polyatomic molecules O_3, CO_2 and H_2O whilst the far infrared absorption (of no consequence to the solar beam but of great importance for the terrestrial (longwave) radiation) is due to purely rotational transitions. The factors primarily determining the atmospheric absorption at a particular frequency are:

(i) the mass absorption coefficient $k_{\nu a}$ and its dependence on ambient temperature and pressure,

(ii) the amount of absorbing constituent traversed by the beam and its distribution along the path,

(iii) the pressure and temperature variation along the beam path.

The determination of the atmospheric transmissivity associated with infrared absorption is complicated by many factors. Foremost among these is the rapid variation of the absorption coefficient $k_{\nu a}$ across the numerous lines of varying intensity which comprise each absorption band. Each line has a finite width resulting from natural damping, collisions and a Doppler effect and the line width is pressure- and temperature-dependent. Because of the complex structure of the absorption bands it is not feasible to work with truly monochromatic transmissivities and a formulation in terms of average values over finite spectral intervals must be invoked: i.e. in terms of

$$\overline{Q}_{\nu,\Delta\nu} = \frac{1}{\Delta\nu} \int_{\nu}^{\nu+\Delta\nu} \exp\left(-\int k_{\nu}\rho \, dr\right) d\nu \quad \ldots(9)$$

the practical object being a functional relationship between $\overline{Q}_{\nu,\Delta\nu}$ and the path-integrated mass of absorber $\int\rho dr (=W)$.

Two approaches are possible:

(i) by adopting certain models of the line and band structure which specify $k_{\nu}(\nu)$ in terms of a small number of parameters and performing the integration of Equation 9,

(ii) by laboratory measurements with a low resolution spectrometer for a range of values of the path-integrated mass of absorber.

In either case the functional relationship $\overline{Q}_{\nu,\Delta\nu}(W)$ is known as a transmission function. The first approach above forms the basis for studies of the longwave radiation in the atmosphere. However, the parameters of the relevant models are as yet not adequately known for the near infrared and the transmission functions for solar radiation are based almost exclusively on experimental data. The fundamental physics being the same it is, however, appropriate to examine the principles of band models before considering the experimental data.

3.4 (i) *Line and band models and theoretical transmission functions*

The band models which have been developed take the form of regular or random arrays of absorption lines of specified shape, spacing and intensity. The individual line shape most frequently employed in the band models follows from the theory of natural broadening or as a simplification of the theory of collision broadening. Known as the Lorentz line shape it is considered realistic below about 40 km in the atmosphere. For the upper stratosphere and above, Doppler broadening assumes significance and the so-called Doppler or a combined Lorentz-Doppler line shape becomes more appropriate. The Lorentz and Doppler shape factors are compared in Fig. 4(a). Corresponding expressions for the mass absorption coefficient are:

$$\text{Lorentz line,} \quad k_\nu = \frac{S}{\pi} \frac{\alpha_L}{(\nu-\nu_o)^2 + \alpha_L^2} \qquad \ldots(10.1)$$

$$\text{Doppler line,} \quad k_\nu = \frac{S}{\alpha_D\sqrt{\pi}} \exp\left(-\frac{(\nu - \nu_o)^2}{(\alpha_D)}\right) \qquad \ldots(10.2)$$

where in both cases S is the line intensity ($= \int_{-\infty}^{\infty} k_\nu \, d\nu$) and the α's are half widths to half intensity which emerge from the respective theories as combinations of certain parameters and physical constants. It is seen that for comparable intensities and half widths the Lorentz line absorbs less in the centre and more in the wings than the Doppler line.

Of the many band models which have been proposed best known are the *regular* (Elsasser) and *random* models. The regular model consists of a number of equally spaced (Lorentz) lines of identical half width and intensity (Fig. 4(b)). In the group of random models the lines, all of identical half width, are distributed randomly over the small spectral interval with their intensities identical, random or specified according to some simple function.

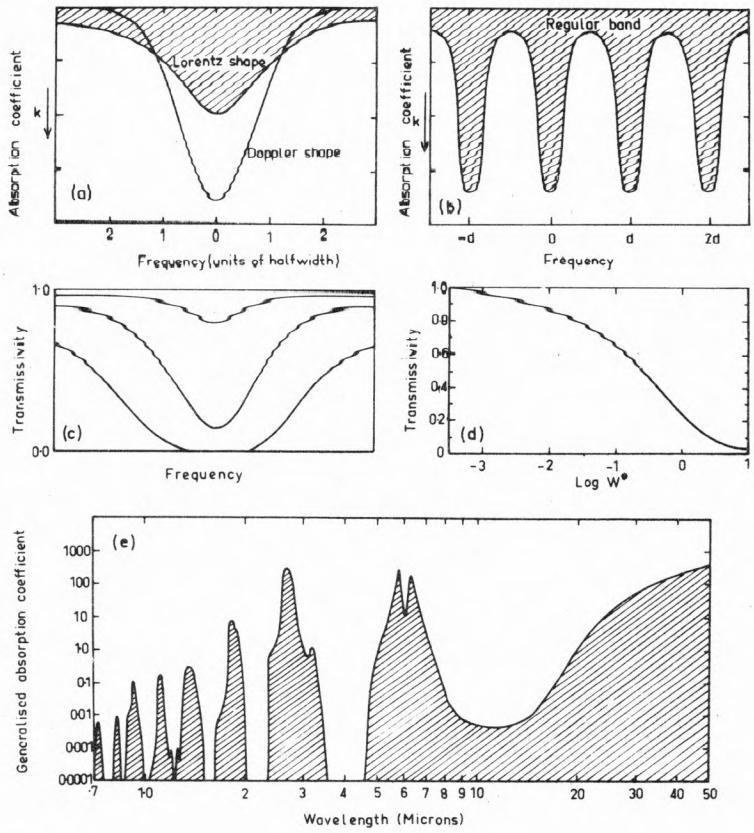

Figure 4

(a) Comparison of Lorentz and Doppler 'line'' shapes for comparable half widths and intensities.

(b) The Elsasser band model.

(c) The variation of tranmissivity across a line for various absorber amounts.

(d) The transmission function for water vapour (Elsasser, 1960).

(e) Schematic generalised absorption coefficient for water vapour (compiled from Yamomoto and Onishi (1952), Elsasser (1960) and Howard et al (1965)).

Assuming a homogeneous path with integrated absorber mass $\int \rho \, dr = W$ the integration of Equation 9 performed for the following simple models,

(a) a single Lorentz line,

(b) an Elsasser band with Lorentz line shape and spacing d,

(c) a random band with Poisson distribution of Lorentz line intensities and average line spacing d,

gives the following forms for the transmission functions along with their "weak" and "strong" approximations.

(a) Lorentz line:

$$\overline{Q}_{\nu,\Delta\nu}(W) = 1 - \frac{2\pi\alpha}{\Delta\nu} x \exp(-x) \left(J_o(ix) - iJ_1(ix)\right) \quad \ldots(11.1)$$

$$\simeq 1 - \frac{SW}{\Delta\nu} \quad \text{for weak absorption} \quad \ldots(11.2)$$

$$\simeq 1 - \frac{2}{\Delta\nu}\sqrt{S \alpha W} \quad \text{for strong absorption} \quad \ldots(11.3)$$

where $x = \frac{SW}{2\pi\alpha}$, the subscript L of α_L has been dropped for convenience and J_o and J_1 are zero and first order Bessel functions (imaginary argument).

(b) Regular band:

$$Q_\nu(W) = \int_y^\infty \exp(-y \coth \beta) J_o(iy/\sinh \beta) \, dy \quad \ldots(12.1)$$

$$\simeq \exp \frac{(SW)}{(d)} \quad \text{a weak line approximation} \quad \ldots(12.2)$$

$$\simeq 1 - \operatorname{erf}\sqrt{\frac{LW}{2}} \quad \text{a strong line approximation} \quad \ldots(12.3)$$

where $\beta = \frac{2\pi\alpha}{d}$ is a measure of line overlapping

$$y = \frac{SW}{d}$$

$L = \frac{2\pi\alpha S}{d}$ is a generalised absorption coefficient.

(c) Randon band:

$$Q_\nu (W) = \exp\left(\frac{-S_o \alpha W}{d\sqrt{\alpha^2 + \frac{S_o \alpha W}{\pi}}}\right) \quad \ldots(13.1)$$

$$\simeq \exp\left(-\frac{S_o W}{d}\right) \quad \text{a weak line approximation} \quad \ldots(13.2)$$

$$\simeq \exp\left(-\frac{\sqrt{\pi S_o \alpha W}}{d}\right) \quad \text{a strong line approximation} \ldots(13.3)$$

where S_o is a parameter describing the mean line intensity.

The physical interpretation of the weak and strong absorption approximations is illustrated in Fig. 4(c). When the product $k_{\nu o}W$ is small ($x<<1$) the absorption continues to increase with increasing W and the linear dependence of 11.2 is valid. For large $k_{\nu o}W$ the centre of the line is soon absorbed away, further absorption can only occur in the wings of a line and subsequent absorption converges towards a square root dependence on absorber mass. Several other models and approximations have been developed and the forms of the resulting transmission functions differ slightly. The Elsasser band model is certainly unrealistic for water vapour and ozone bands but not too bad for carbon dioxide. In principle, the theoretical transmission functions require only spectroscopic determination of the relevant model parameters (line intensity, spacing and perhaps also half-width) to render them explicit functions of the path integrated mass W. In practice, particularly for the near infrared spectrum these parameters are not yet adequately known and determination of the transmission functions is based on low resolution spectrometry.

3.4 (ii) Laboratory transmissions

The approximation forms for the band model transmission functions of Equations 12 and 13 suggest that in general laboratory transmission functions may be determinable in a form $Q_\nu = Q_\nu (L \cdot W)$ where the functional *form* of Q_ν will not vary with frequency and the unresolved band structure may be specified in terms of the generalised absorption coefficient L. For a particular gas and using a convenient frequency band the transmissivity is measured for a series of values of W and the transmission function determined empirically. Its form for water vapour is illustrated in Fig. 4(d). Variation of generalised absorption coefficient L over the band is then simply found from the displacement of the transmission function curves along the log W scale of Fig. 4(d) for successive frequency intervals. Fig. 4(e) shows schematically the generalised absorption coefficient for the principal infrared water vapour bands.

Given the transmission functions for the various atmospheric constituent gases and their corresponding generalised absorption coefficient L from wide-slit laboratory data it would seem a trival problem to compute the spectral (and integral) absorption of the solar beam in terms of the mass of absorber present in the atmosphere. Unfortunately from the point of view of computation, pressure and temperature conditions vary along the solar beam path whilst the laboratory data are obtained for homogeneous absorber paths at specified pressure and temperature. Now, since the theory of line broadening predicts and experiment confirms that for a given absorber mass the transmissivity is pressure- (and to a lesser degree, temperature-) dependent some method of allowing for this when applying the laboratory data in atmospheric studies must be devised. One approximate method simulates the (real) non-homogeneous path by a homogeneous path containing a scaled mass of absorbing material W*. In this formulation $W^* = \int P_S \rho \, dr$ where P_S is the scaling parameter for which many forms have been derived and which of course is different for different absorbers. For water vapour $P_S = \frac{p}{p_o} \left(\frac{T_o}{T}\right)^{\frac{1}{2}}$ has been frequently used.

Figs. 3(c), (d) and (e) show for *scaled* absorber amounts of 0.30 cm of ozone (NTP), 100 cm of carbon dioxide (NTP) and 1 cm of precipitable water vapour (realistic estimates for a middle latitude atmosphere) the corresponding zenith beam transmissivities. They indicate what fraction of the vertically incident solar beam at the various wavelengths would penetrate to the surface if each absorber alone were acting. Data are given also for the far infrared spectrum. In this case they indicate what fraction of the *vertical* emitted intensity at the earth's surface will be received by a high resolution satellite sensor viewing the sub-satellite point.

3.5 The solar spectrum at sea level

For the model atmosphere assumed in the previous sections, i.e. with an Angström turbidity coefficient of 0.100, a pressure at sea level of 1000 millibars, and scaled or "effective" contents of 0.3 cm (NTP) ozone, 100 cm (NTP) of carbon dioxide and one centimetre of precipitable water, the atmospheric transmissivity at a particular wavelength which is the product of the individual transmissivities is as shown in Fig. 3(f). Fig. 3(g) shows the corresponding solar spectrum after depletion. It accords closely with measured solar spectra. The extra-terrestrial solar beam spectral distribution is included for comparison. It is seen that the direct solar radiation at sea level contains no significant energy below 0.3μ due to the strong ozone absorption and molecular scattering. Molecular and aerosol scattering are mainly responsible for solar beam depletion in the visible. A few weak water vapour bands (the "rain" bands) contribute negligibly. Depletion in the infrared is due principally to a number of intense water vapour bands and two partially overlapped carbon dioxide bands. A contribution also arises from three oxygen bands at 0.69μ, 0.76μ and 1.25μ not shown here.

Fig.3, it should be noted, apart from considering one particular combination of absorbers is constructed for a *vertical* solar beam so that the transmissivities are in fact the q's introduced earlier. For the sun at other elevation h above the horizon the transmissivity is given via Equation 4.2: $Q_\nu = (q_\nu)^{m_r}$ where the relative optical path m_r is to a close approximation equal to cosec h for each depleting medium.

3.6 Solar heating of the atmosphere

The atmosphere is heated by absorption of the solar beam by the ozone, carbon dioxide, water vapour and other minor absorbers. The vertical distribution of solar beam heating is determined primarily by the distribution of absorbing material, its absorption function, the ambient density and the solar zenith angle. The atmosphere is also heated by absorption of the partly diffused shortwave radiation reflected from the clouds and ground and scattered out of the solar beam by the cloudless atmosphere. The atmospheric heating due to absorption of scattered and reflected radiation may amount to a sizeable fraction of the whole.

Consider absorption of the *direct solar beam* in a cloudless atmosphere. The rate of temperature rise at some arbitrary level z is given by:

$$\frac{\partial T_z}{\partial t} = - \frac{1}{\rho_z c_p} \nabla \cdot \underset{\sim}{S_z} \qquad \ldots(14)$$

where $\underset{\sim}{S_z}$ is the solar beam irradiance vector after penetration to the level z.

Now for any spectral interval (or the entire solar spectrum by combining mean transmissivities for the several bands with data on the extra-terrestrial relative spectral irradiance) since $S = S_E\, Q\, (W_z^*)$ and $W_z^* = w_z^* / \cos\zeta$ where w_z^* is the scaled mass of absorber above level z measured vertically and ζ the solar zenith angle, we have for the instantaneous rate of heating

$$\frac{\partial T_z}{\partial t} = \frac{S_E}{\rho_z c_p} \frac{\partial}{\partial z} \left(Q \frac{(w_z^*)}{(\cos\zeta)} \cdot \cos\zeta \right) \qquad \ldots(15.1)$$

For most purposes we wish to filter out the diurnal cycle and assess mean daily heating rates. This is achieved by

integrating Equation 15.1 from sunrise to sunset or by the approximate device of rewriting Equation 15.1

$$\text{as} \quad \overline{\left(\frac{\partial T_z}{\partial t}\right)}_{\text{day}} = r \frac{S_E \cos \bar{\zeta}}{\rho_z c_p} \cdot \frac{\partial}{\partial z} \left(Q \left(\frac{w^*}{\cos \bar{\zeta}} \right) \right) \qquad \ldots(15.2)$$

where r is the fraction of the day during which the sun is above the horizon and $\bar{\zeta}$ is a mean zenith angle defined by

$$\bar{\zeta} = \arccos \left(\int_{\text{sunrise}}^{\text{sunset}} \cos \zeta \, (t) \, dt \Big/ \int_{\text{sunrise}}^{\text{sunset}} dt \right)$$

It is frequently necessary to compute the mean solar heating rate for particular atmospheric layers. Transforming to pressure coordinates and introducing appropriate numerical values it is, for mean sun earth distance and $p_2 - p_1$ in millibars:

$$\left(\frac{\partial T}{\partial t}\right)_{\substack{\text{layer} \\ p_1 - p_2}} = \frac{11660 \cos \zeta}{p_2 - p_1} \left[Q\left(\frac{w_{p_1}^*}{\cos \zeta}\right) - Q\left(\frac{w_{p_2}^*}{\cos \zeta}\right) \right] {}^{\circ}\text{C per day} \qquad \ldots(15.3)$$

Practical use of Equations 15.2 and 15.3 necessitates a knowledge of Q(W*) for the particular absorber. *Integral* solar beam transmissivity curves for ozone, carbon dioxide and water vapour based on recent data on the extra-terrestrial solar spectrum (Fig. 3(a)) and laboratory absorption measurements are given in Fig. 5.

A number of authors have computed the vertical distribution of direct solar beam heating for cloudless skies and various model distributions of the absorbing constituents. The total heating rate is the sum of the heating rates due to the individual absorbers reduced by a small amount to allow for counting twice absorption in overlapping bands. Fig. 6 shows a synthesised pole to pole cross section of total heating due to all significant infra-red bands. The strong high level heating due to ozone absorption is not included. The calculations were by Yamomoto (1962). His choice of scaling parameter and absorber distribution is given in his paper.

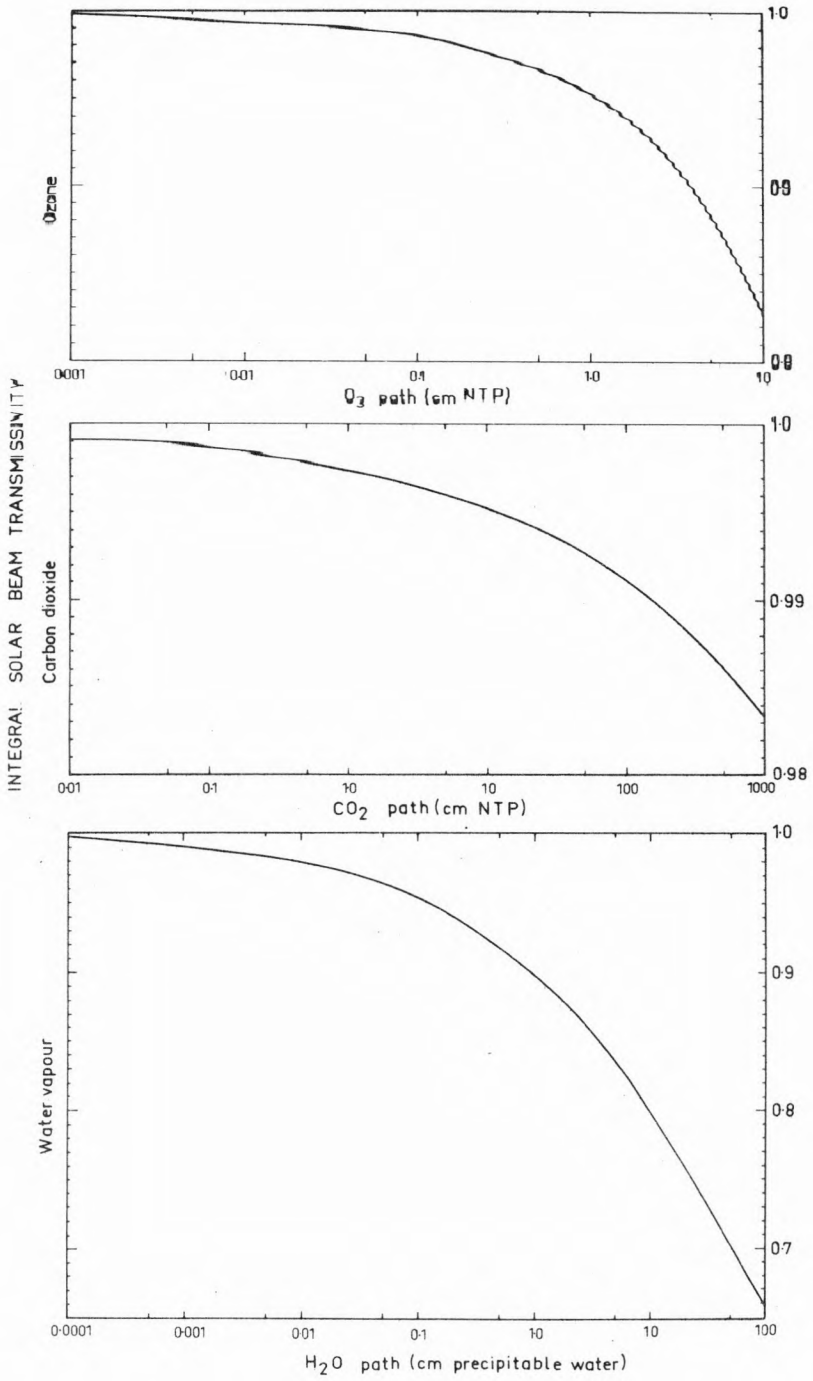

Figure 5. Integral solar beam transmissivity for various scaled or 'effective' paths of ozone, carbon dioxide and water vapour (compiled from Manabe and Möller (1961)).

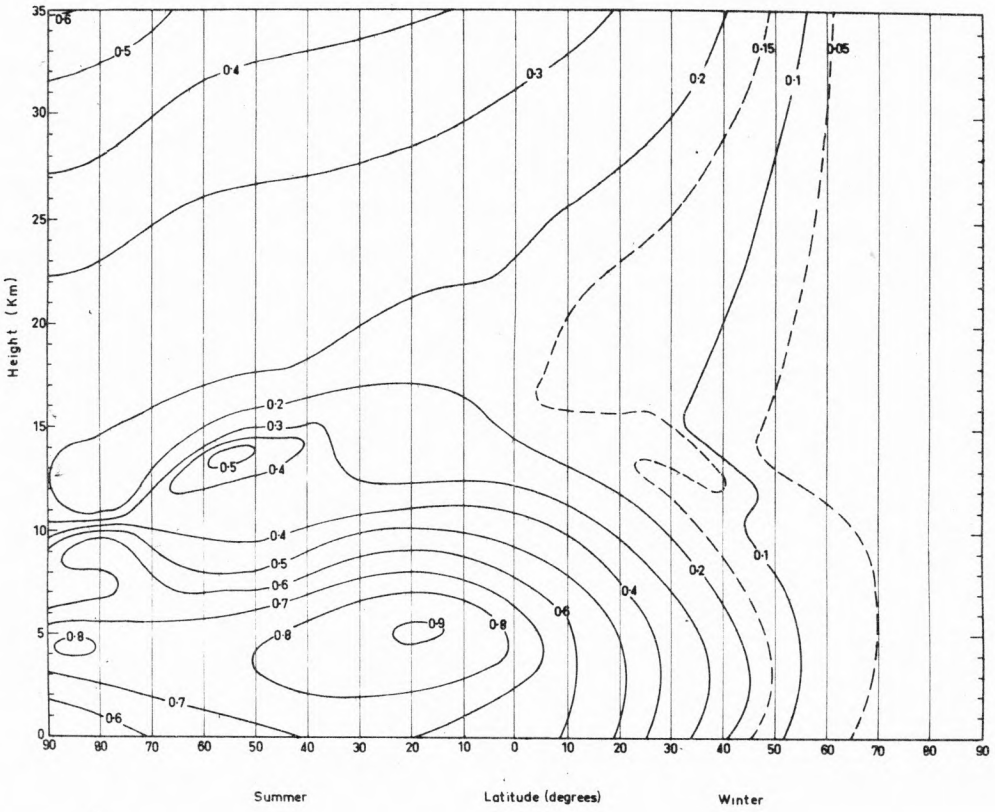

Figure 6. Distribution with latitude and height of absorption heating ($^{\circ}$C per day) in a cloudless atmosphere due to infrared solar radiation absorption by water vapour, oxygen and carbon dioxide (Yamomoto (1962) – northern hemisphere data).

Neither the absorption of scattered and reflected radiation nor the influence of clouds is incorporated in Fig. 6. Fig. 7 adapted from Manabe and Strickler (1964) presents heating rates computed for a model atmosphere containing mean (Northern Hemisphere) cloudiness according to a scheme which allows for absorption of cloud- and ground-reflected radiation but not the Rayleigh scattered component. The large heating rates in the stratosphere result from the inclusion also of solar ultraviolet absorption.

Some idea of the relative importance of the three principal absorbers, ozone, carbon dioxide and water vapour, in the hemisphere-average heating rates may be gained from Fig. 8. Direct beam heating only was considered and cloudless conditions assumed. The curves labelled S refer to the solar absorption. The computations were by Manabe and Möller (1961). The L curves refer to longwave radiation effects ; their significance is examined later.

3.7 Solar heating of the earth's surface

Ultimately of greater significance to the behaviour and structure of the atmosphere than its heating through direct absorption of solar radiation is its energy supply through non-radiative processes at its lower boundary. This surface energy source results largely from the absorption by the ground, water or ice of the shortwave radiation which has penetrated to ground level. The net solar radiation absorbed at the surface is

$$R_S = S_G (1 - \alpha_G) \qquad \ldots(16)$$

where S_G known as the global radiation has two components, the vertical part of the direct solar beam and the diffuse sky radiation; i.e.

$$S_G = S \sin h + D \qquad \ldots(17)$$

Its determination on various time scales is a matter of considerable importance to both diagnostic and prognostic branches of meteorology as well as to many related disciplines. α_G is the albedo of the surface for the global radiation and is a complex function of many variables most notably the type of underlying surface and solar elevation angle. Its practical determination is invariably empirical and numerous texts contain tables of global radiation albedo for a variety of surface types.

The global radiation may be measured directly using thermal or thermoelectric sensing devices known as pyranometers. This is possible, however, only at a sparse network over the world and computational methods have been developed to fill in the gaps. Also values for the shortwave income at the surface must be amenable to parameterisation for use in theoretical forecasting by mathematical models.

The most sophisticated methods for determination of the global radiation invoke wavelength integrations of the spectral absorption and scattering characteristics of the atmosphere to determine the direct component and the theory of multiple scattering for the diffuse component. The most frequently used are simple one or two parameter empirical relations.

For a cloudless atmosphere with high sun, between 60% and 85% of the undepleted insolation reaches the earth as global radiation. This fraction, known as the relative insolation, is strongly dependent on solar elevation and water vapour content of the atmosphere. For assumed mean aerosol content its value over the southern hemisphere oceans is given approximately in terms of solar elevation and surface dewpoint in Fig. 9. The global radiation follows by multiplication with S_E sin h. For a simple approximate estimate of the clear sky global radiation in low and middle latitudes the relationship

$$S_{Go} = 16\ h \text{ watts metre}^{-2} \qquad \ldots(18)$$

may be used for solar elevation $<55^o$ (h in degrees). Daily average values of the global radiation for cloudless skies based partly on direct measurement and partly on computation have been summarised as zonal means (on a monthly basis) for the world by USSR investigators. Southern Hemisphere values are given in Fig. 10.

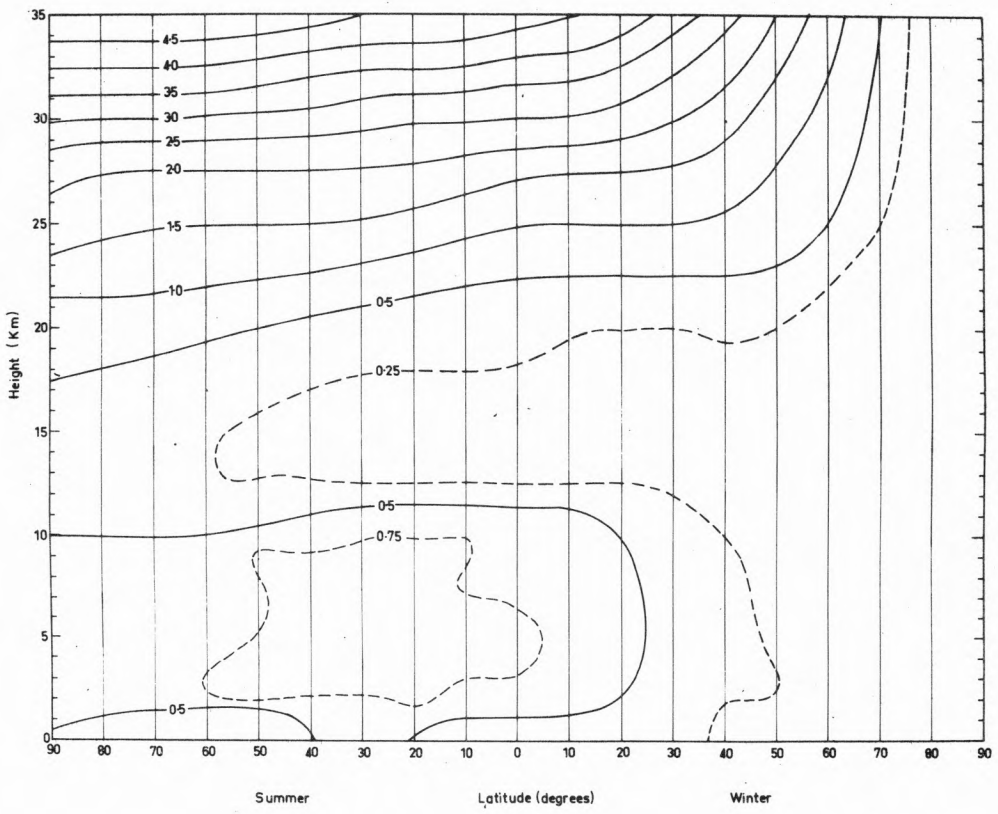

Figure 7. Distribution with latitude and height of absorption heating ($^{\circ}$C per day) due to solar radiation absorption by cloud, water vapour, ozone and carbon dioxide (Manabe and Strickler (1964) – northern hemisphere data).

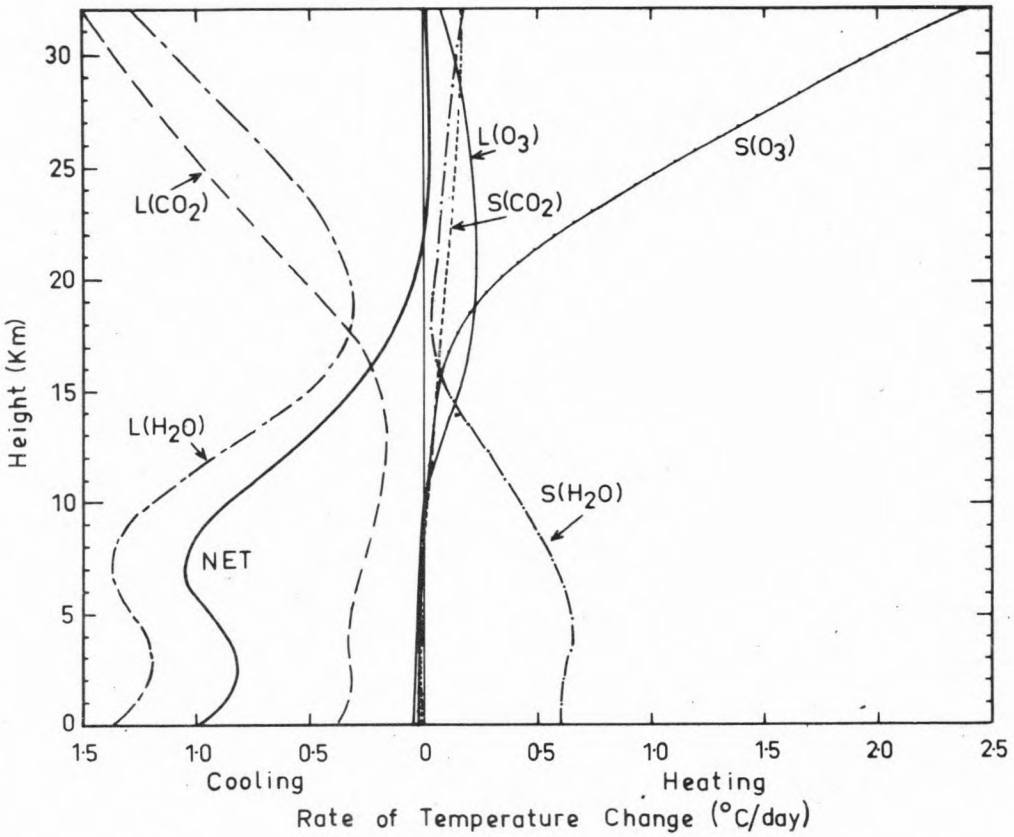

Figure 8. Vertical distribution of heating and cooling (°C per day) due to shortwave (S) and longwave (L) radiation absorption and emission by water vapour, carbon dioxide and ozone. Hemispheric average values from Manabe and Möller (1961).

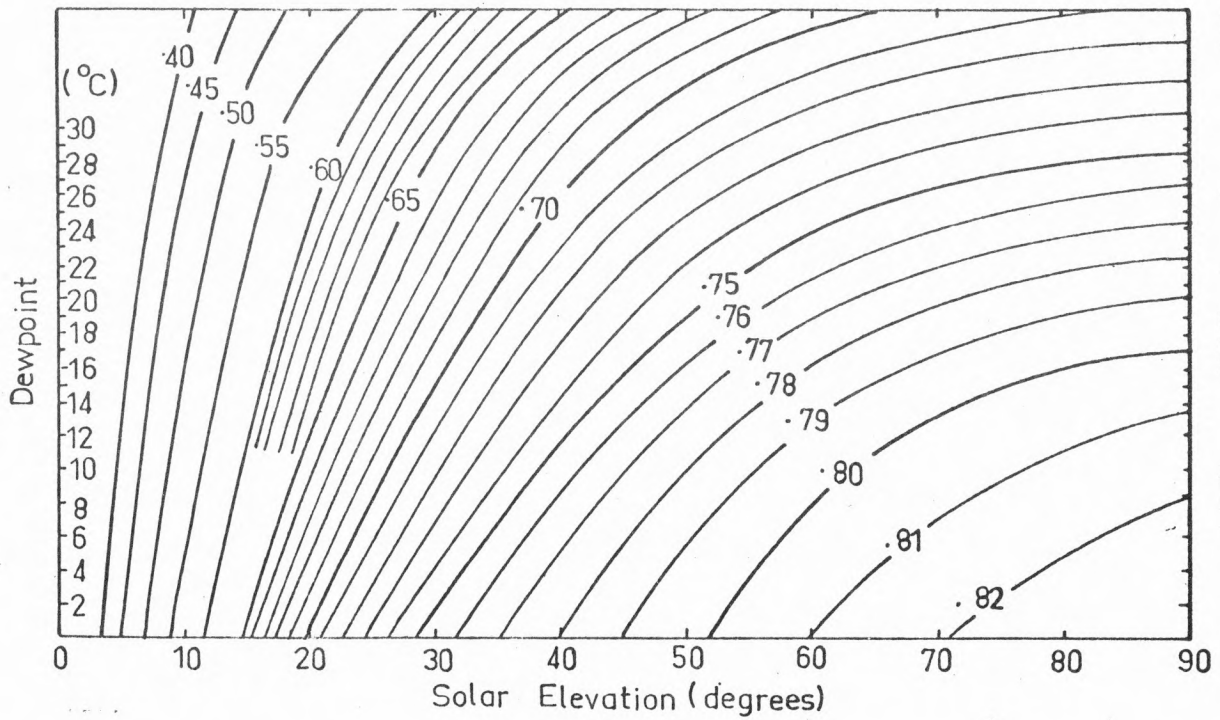

Figure 9. Nomogram for approximate determination of cloudless sky relative insolation as a function of solar elevation and surface dewpoint based on the theoretical method of Schüepp (1966) and surface dewpoint – precipitable water – turbidity relationships appropriate to the southern hemisphere oceans.

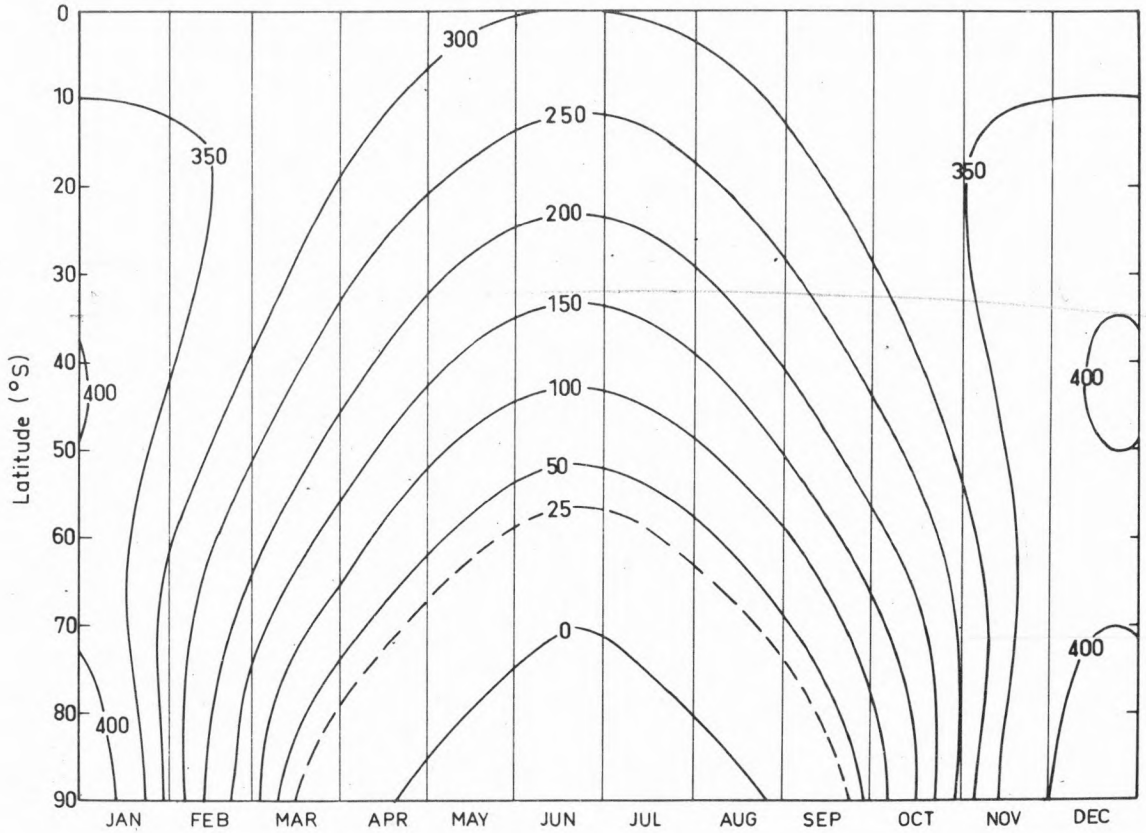

Figure 10. Latitude and seasonal distribution of monthly mean global radiation (watts metre $^{-2}$) with cloudless skies for the southern hemisphere. (Prepared from data given by Kondratyev (1969) after Berland (1962)).

By far the most significant meteorological factor influencing the global radiation at the earth's surface is the cloud cover. For short periods the tremendous variability in cloud type and opacity precludes exact calculation of the global radiation but for extended time periods (a month or so) simple empirical relations of linear or quadratic form prove useful in deriving mean values of global radiation from undepleted or equivalent clear sky values and corresponding values of mean fractional cloudiness. Probably the most widely applicable empirical formula of this type is that given by Berland (1960), viz.

$$S_G = S_{Go} \ (1 - bC - 0.38C^2) \qquad \ldots(19)$$

where S_{Go} may be read from Fig. 10. C is fractional cloud cover on a scale 0-1 and b is a function of latitude whose value is 0.35 at lat. 25^o and 0.38 at latitudes 35^o and 45^o. The annual mean distribution of global radiation for the southern hemisphere determined principally on the basis of Equation 19 and climatic mean cloudiness estimates is shown in Fig. 11.

4. THE RESPONSE OF THE ATMOSPHERE

4.1 Atmospheric heat balance and circulation

We have seen that the sun is continuously supplying energy to the earth's surface and its atmosphere and the rate of solar energy input is dependent on latitude and season; over a complete year the total solar radiation heat income to the equatorial regions is considerably greater than to the poles. We observe the atmosphere to be a viscous fluid maintained in continual motion with respect to a constantly rotating earth. We conclude that, since the planet as a whole is not steadily getting warmer, nor, in the annual mean is any latitude or level heating differentially, and neither is the circulation of the atmosphere running down nor any other known energy reservoir being built up or depleted, there are processes at work which ensure that:

(i) as much heat leaves the earth-atmosphere system as arrives from the sun,

(ii) as much heat escapes to space from each latitude band as that band receives from the sun or else an internal exchange is occurring in which the equatorial regions make up the relative deficit of the poles,

(iii) the atmospheric layers where strong solar absorption heating occurs are strongly cooled by the other heat exchange mechanisms and the weakly solar-heated layers correspondingly weakly cooled,

(iv) in the complex cycle, which involves receipt of vast amounts of thermal energy from the sun, its storage, conversion and redistribution in the atmosphere and oceans and its ultimate return to space, a small amount is made available to restore the kinetic energy which the atmosphere loses by irreversible frictional dissipation and so in effect to drive the atmospheric heat engine.

We will now examine, first for the planet as a whole and then for individual latitude bands the processes which maintain the observed thermal structure of the atmosphere against the solar heating and then the part which the solar heating itself plays in maintaining the atmospheric circulation.

4.2 The planet in radiative balance

If S_E = the incident power per unit area normal to the solar beam outside the atmosphere

α = the mean albedo of the planet ($\simeq 0.30$ (Raschke, 1968))

πr_e^2 = the cross sectional area of the earth intercepting the solar beam

$4\pi r_e^2$ = the total area of the earth's surface,

the total solar power absorbed by the planet is $(1 - \alpha)\, S_E\, \pi r_e^2$ ($\simeq 1.23 \times 10^{17}$ watts) and the average power per unit area of the earth's surface $\frac{(1 - \alpha)}{(4)} S_E$ approximately 240 watts metre^{-2}.

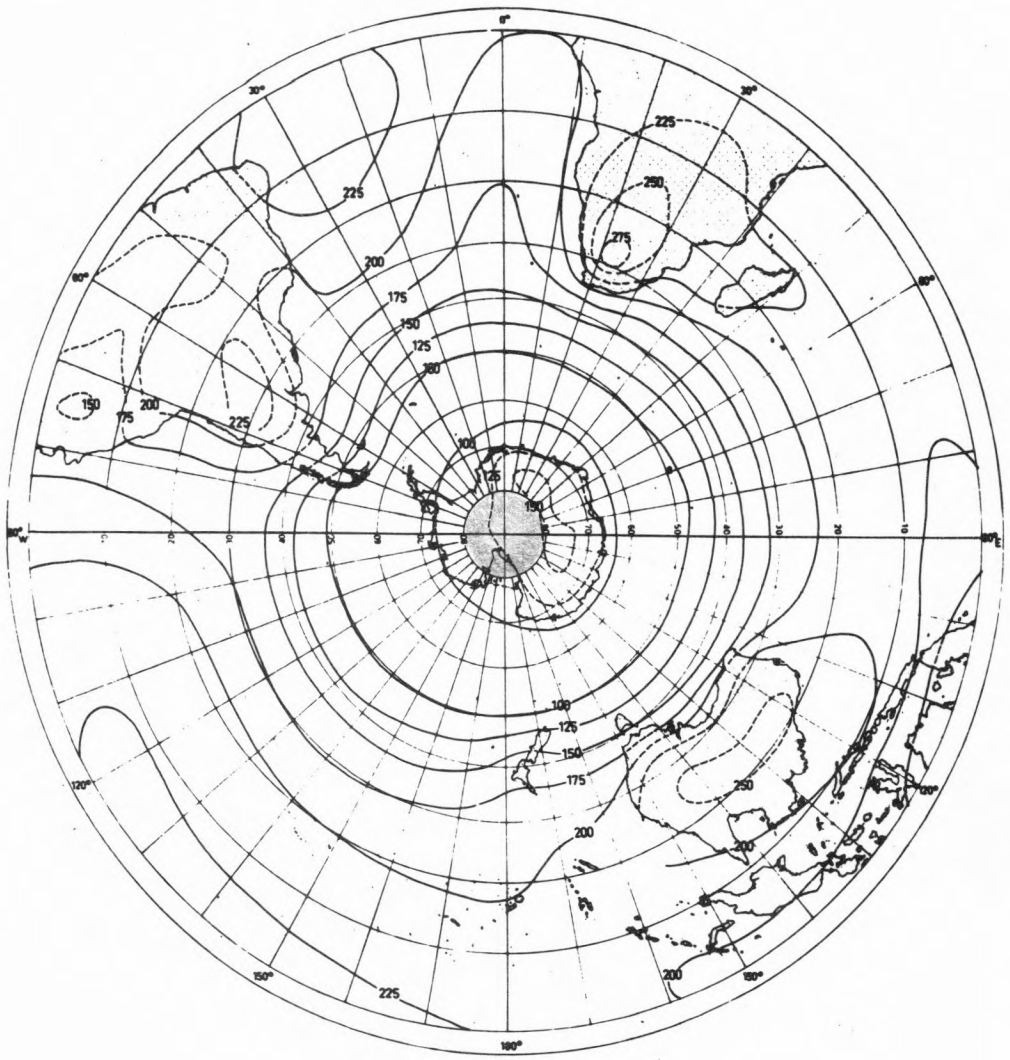

Figure 11. Annual mean global radiation (watts metre^{-2}) reaching the surface of the southern hemisphere. (Compiled from Budyko (1963), Braginskaya et al (1966) and Zillman (1967)).

Since this energy does not continue to accumulate in any known form (internal, gravitational potential, kinetic, chemical ...) in the earth-atmosphere system it must be returning to space at the same rate, and since there is no intervening medium the transfer must be by thermal radiation.

If the planet is approximated to a black body radiator with a radiant emittance of σT^4 we may immediately compute the temperature T from

$$T = \left(\frac{(1 - \alpha)\ S_E}{4\sigma}\right)^{\frac{1}{4}}$$

It turns out to be 255°C, some 30°C lower than the mean temperature of the earth's surface. This is consistent with our observation that the atmosphere is only partially transparent to terrestrial radiation and so a part of the planetary radiant emittance originates in the colder high troposphere. By analogous reasoning we find planetary radiative temperatures of 217°K for Mars (albedo 0.16) and only 32°K for the large outer planet Neptune (albedo 0.84).

4.3 Meridional radiative imbalance of the earth-atmosphere system

As a dual consequence of sun-earth geometry and the relatively high albedo of the polar regions the annual solar radiant income to the atmosphere-earth system decreases from the equator to the poles as shown in Fig. 12. If the atmosphere and ocean were constrained to prevent internal heat flow across latitude circles with each latitude band in the annual mean in radiative balance with space the effective radiative temperature $T = \left(\frac{S_{VE}}{\sigma}\ (1 - \alpha)\right)^{\frac{1}{4}}$ would decrease from about 265°C at the equator to 190°C at the poles. In reality as anticipated from theoretical considerations and confirmed recently by satellite measurements the longwave radiation leaving the polar regions is much greater than the shortwave radiation absorbed, whilst in the tropics the absorbed shortwave exceeds the longwave loss. The absorbed shortwave excess, the radiation imbalance, ranges in the annual mean from positive values of about 40 watts metre^{-2} near the equator to negative values of nearly 100 watts metre^{-2} at the poles. To maintain the observed state of annual heat balance the equatorial excess must be transferred within the earth-atmosphere system to make up the deficit at the poles. The poleward

transfer across latitude circles required to effect this balance is shown in the bottom part of Fig. 12.

4.4 Radiative imbalance of the atmosphere

Though it has just been shown that individual latitude bands of the earth-atmosphere system are not in radiative equilibrium with space (in the annual mean) no attempt was made to partition the resulting necessary heat transfer across latitude circles between the atmosphere and oceans and the possibility that the atmosphere, or at least a part of it, is in radiative equilibrium has not yet been ruled out.

For radiative equilibrium to prevail in the atmosphere the solar-absorption-heating (Figs.6 and 7) must be exactly offset by cooling due to divergence of the net longwave flux. The latter is a function of the vertical distribution and temperature of the absorbing constituents (water vapour, carbon dioxide and ozone principally) and the temperature and emissivity of the underlying surface. It may be determined by direct measurement (radiometersondes, limited data so far) or computational schemes (radiation charts) based on integral forms of the equation of radiative transfer with Planckian source function and laboratory transmissivity data for the atmospheric constituents.

The possibility that the observed thermal structure of the atmosphere represents a state of balance between the short-wave heating and a net longwave cooling may be examined in either of two ways:

(i) The observed distribution of (short and longwave) absorbing and emitting constituents together with appropriate boundary conditions is used to compute an equilibrium temperature structure and this compared with the observed temperature field,

(ii) The difference between the solar heating and a longwave cooling rate appropriate to the observed temperature structure is assessed and taken as an index of departure from radiative equilibrium.

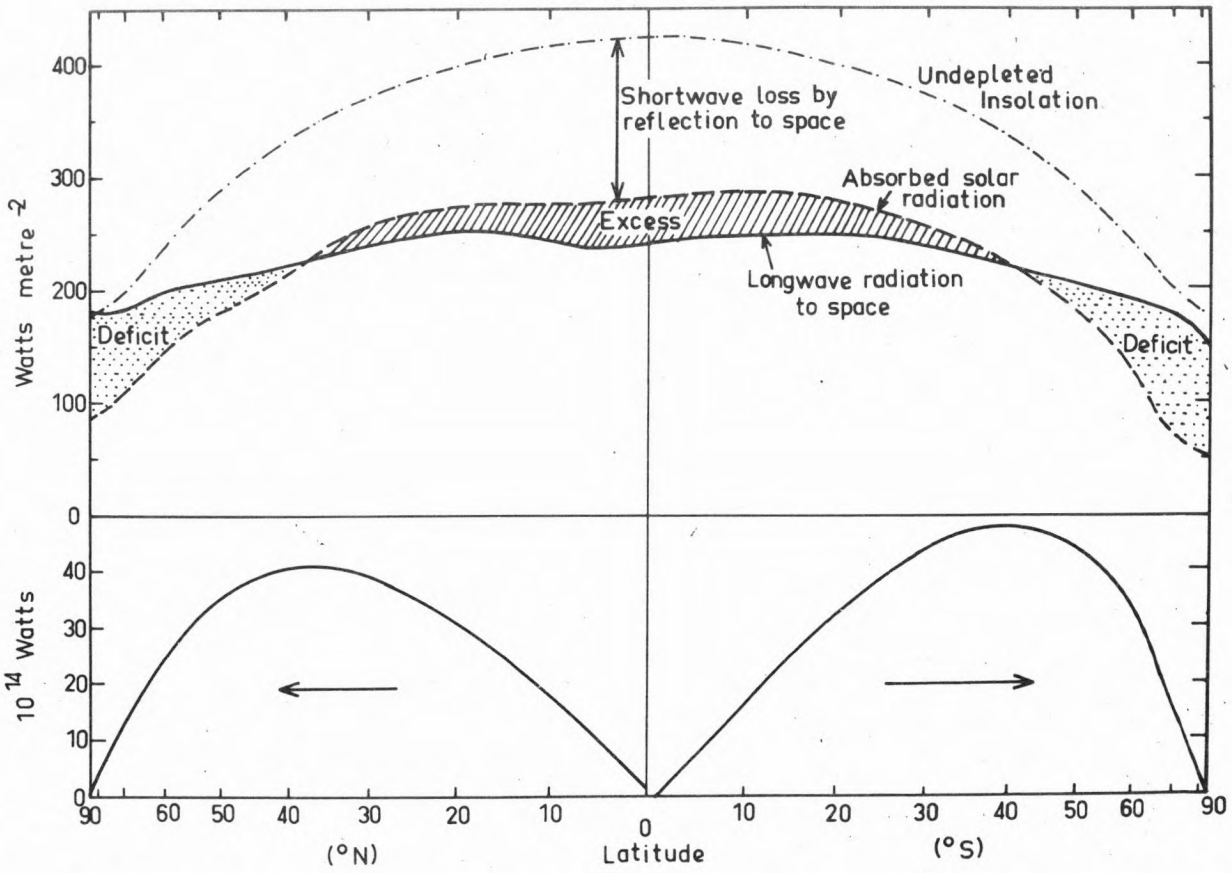

Figure 12. Heat balance of the earth–atmosphere system showing annual mean values of the undepleted insolation, absorbed shortwave radiation and longwave emission to space as a function of latitude. The net radiant heat gain by the earth–atmosphere system in the equatorial regions is shown hatched and the polar deficit stippled. The internal heat transfer across latitude circles required for balance is shown in the lower part of the diagram. The latitude scale provides an equal area representation for all latitudes.

In the simplest variants of the first approach a single atmospheric absorber (water vapour) exponentially distributed in the vertical is assumed to radiate as a grey body and the vertical temperature profile consistent with surface black body emission equal the surface shortwave absorption computed on the basis of the equation of radiative transfer. The result is an exceedingly steep lapse rate near the surface decreasing with height to give isothermal conditions above 10-15 kilometres (Fig. 13(a)). Early explanations of the tropopause (e.g. Emden 1913) invoked the resulting static instability near the surface to transport heat upwards, the convection regime giving way to radiative equilibrium above the level of penetration of the rising buoyant parcels of air.

This simple model fails to account for the observed latitudinal variation of the height of the tropopause and the temperature of the ~~strato~~sphere but with subsequent refinements which are of detail rather than principle provides a remarkably adequate description of the *gross* features of the atmospheric thermal structure. The refinements are several:

(a) inclusion of additional longwave absorbers (notably CO_2 and O_3) and much improved knowledge of their vertical distribution,

(b) inclusion of solar absorption heating by CO_2 and O_3 as well as H_2O,

(c) non grey absorption,

(d) allowance for temperature and pressure effects and band overlapping.

A number of extremely important recent studies incorporating these and additional refinements and numerous combinations of distributions and total amounts of the various absorbers have been made using both iterative techniques to approach equilibrium from an initial isothermal state and matrix methods to solve sets of homogeneous equations for the equilibrium thermal structure. Fig. 13(b) after Manabe and Strickler (1964) compares the radiation equilibrium temperature profile for H_2O, CO_2 and H_2O + CO_2 + O_3 absorbing atmospheres under cloudless conditions at 35^oN in April with the U.S. standard atmosphere. It is seen that with the inclusion of ozone absorption a tropopause appears near 10 kilometres. However, lapse rates in the lower atmosphere are, as with the simpler model, far too great and the surface temperature far too warm. With the inclusion of a

"convection adjustment" in the computational scheme whereby an upper limit of $6.5^{o}C\ km^{-1}$ is set for the lapse rate an equilibrium profile (Fig. 13(c)) results with the tropopause rising to 13 km and a more realistic surface temperature. Inclusion of cloud layers at various levels and realistic adjustment of total amounts of the various absorbers results in relatively small variations in the form of the equilibrium profile.

The conclusion from these studies is that whilst an assumption of pure radiative equilibrium correctly indicates the gross features of the atmospheric thermal structure there are several very important deficiencies:

(a) tropospheric lapse rates are unrealistically large,

(b) the complex meridional variation of stratospheric temperature is not reproduced,

(c) the predicted poleward descent of the tropopause is too small.

Conclusions from the second type of study bear out the radiative equilibrium calculations. A particularly interesting set of results is contained in Fig. 14 and Fig. 8. Fig. 14 shows the computed annual mean rate of radiative temperature change. It is seen that net radiative cooling exists at all levels in the troposphere, and in the stratosphere poleward of 35^{o}. It is evident that heat transfer processes other than radiation must make up this deficit. Fig. 8 illustrates for annual and hemispheric mean conditions the contribution of the various atmospheric absorbers to the large negative radiative *imbalance* of the troposphere and the near balance of the stratosphere.

4.5 Atmospheric heat balance

Having established that in general radiation balance does not prevail in the atmosphere we seek to identify the heat sources which make up the deficit. For simplicity let us ignore the vertical variation of radiative imbalance and examine the meridional variation of net radiative heat deficit of the entire layer from the surface to 30 km or more. In the annual mean it is as shown in Fig. 15. The remarkable aspect is the slight latitudinal variation with relative minima around $50\text{-}60^{o}$ north and south and maxima at higher latitudes. These features and

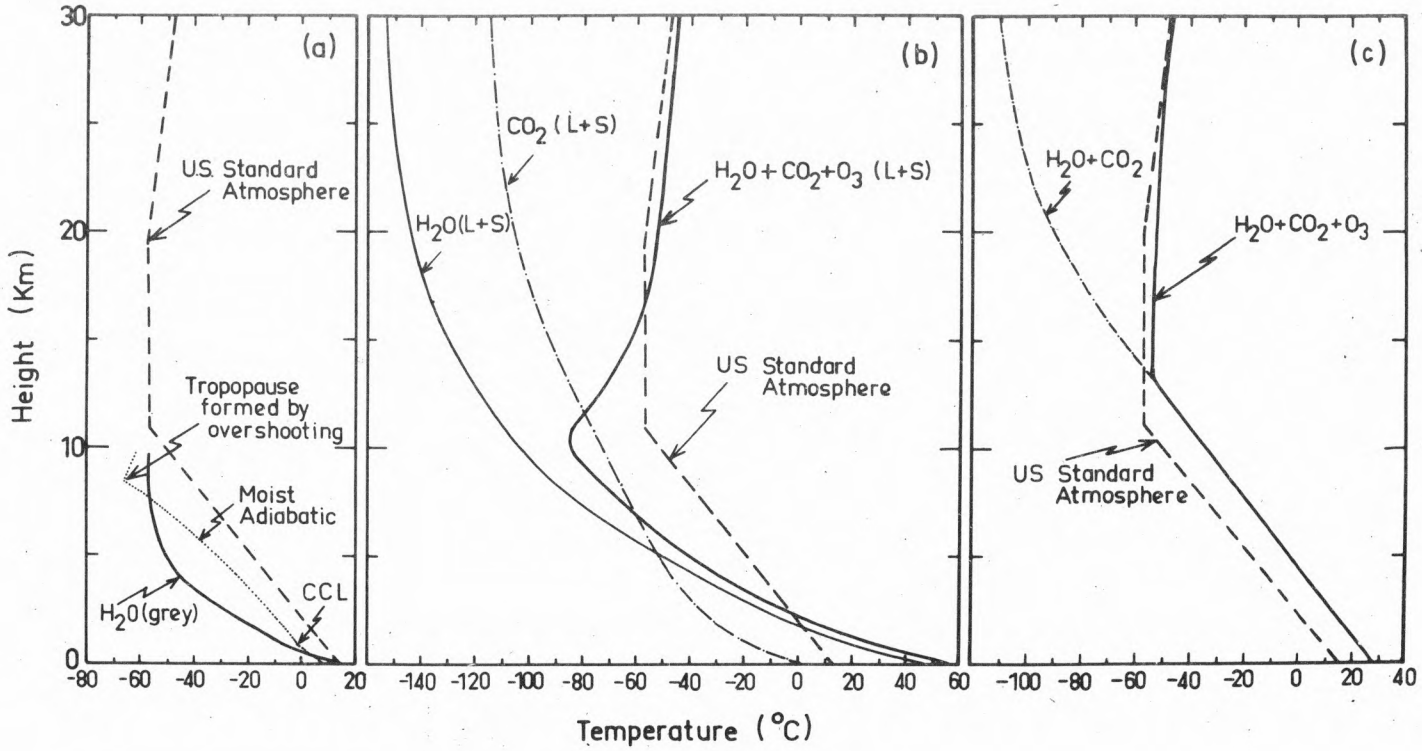

Figure 13. Radiative equilibrium approaches to the thermal structure of the atmosphere:

(a) the approach of Emden (1913) with grey absorption by water vapour initiating superadiabatic lapse rates.

(b) pure radiative equilibrium profiles for water vapour and carbon dioxide absorption separately and together in conjunction with ozone: for cloudless conditions and distribution of gaseous absorbers appropriate to 35°N in April (Manabe and Strickler, 1964).

(c) thermal equilibrium for $H_2O + CO_2$ & $H_2O + CO_2 + O_3$ atmospheres which have a critical lapse rate of 6.5° per Km: conditions as for (b) (Manabe and Strickler, 1964).

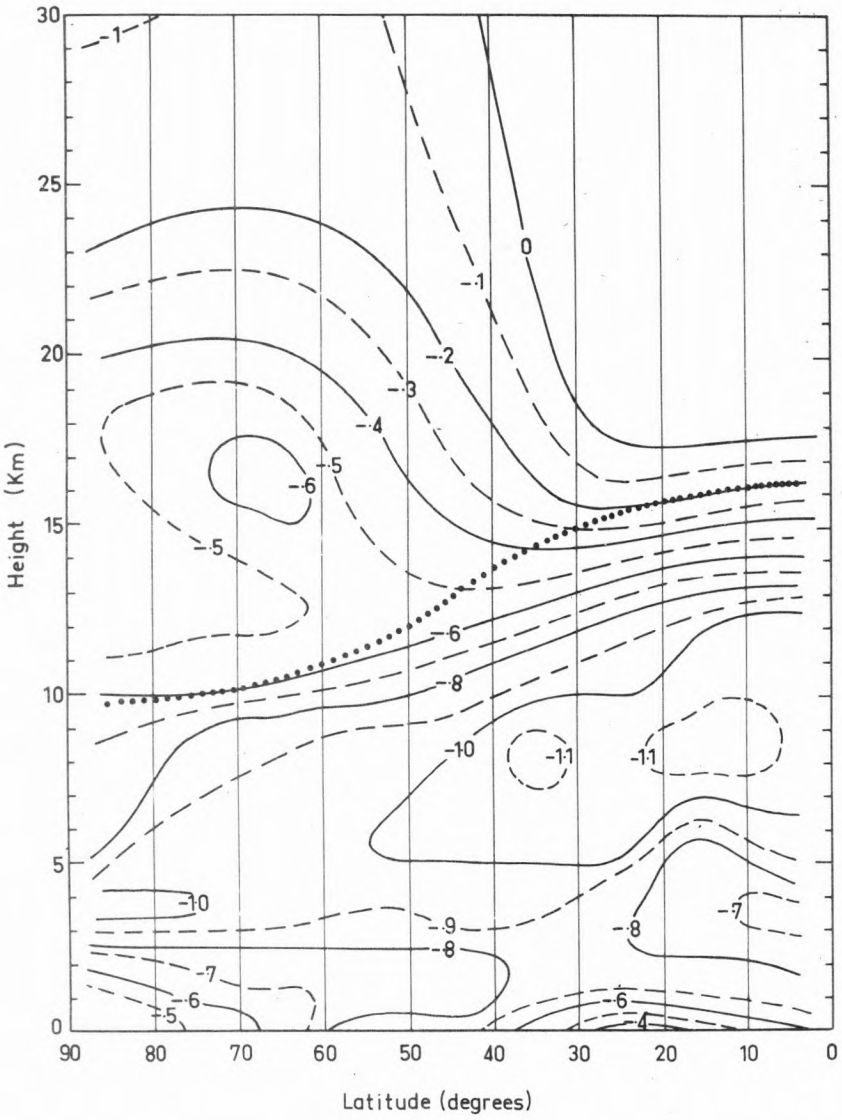

Figure 14. Distribution with latitude and height of annual mean rate of net radiative temperature change ($^{\circ}$C) per day) based on northern hemisphere data. (Manabe and Möller, 1961).

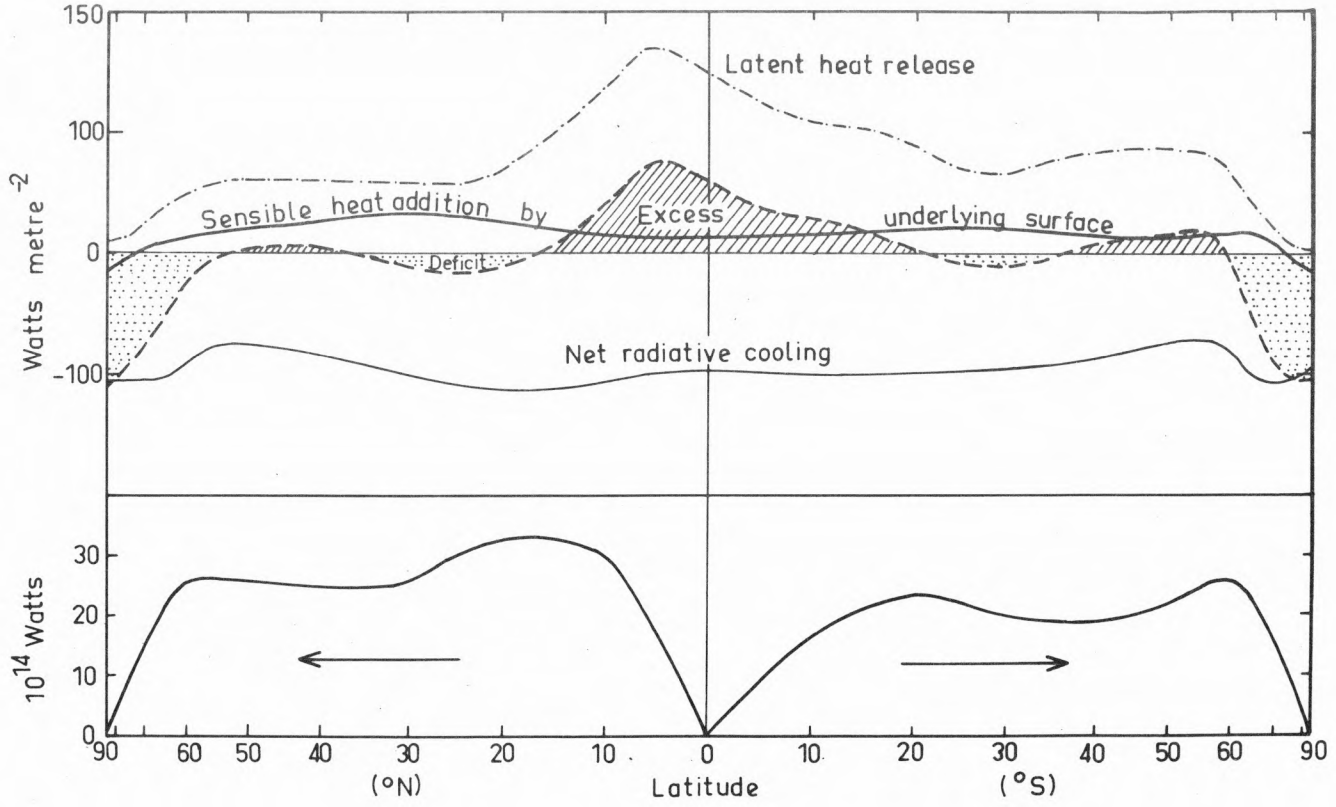

Figure 15. Heat balance of the atmosphere showing the net radiative cooling, the latent heat release by water vapour condensation and the net transfer to the atmosphere of sensible heat from the underlying surface. The transfer across latitude circles within the atmosphere required to effect a balance between the latitudinally distributed heat sources and sinks is shown in the bottom part of the diagram.

their magnitudes are based on recent theoretical and empirical computations as well as limited satellite data but are only just beyond the limits of uncertainty for the various estimates. Fig. 15 includes also the mean annual latitudinal variation of the heat sources which at some latitudes overcompensate and at other latitudes fail to make up for the radiation deficit. Most important is the latent heat release by condensation of water vapour which has been evaporated from the oceans and carried upwards by turbulence and broadscale ascent. Of secondary importance is the heat addition due to the passage of air over warmer underlying surfaces. So the net result of the radiant, latent and sensible heating and cooling of the atmosphere is a heat excess over the tropics and the polar oceans with deficits over the subtropics and both polar ice sheets. The constraint of annual heat balance requires a transport of heat across latitude circles within the atmosphere and this is as shown in the bottom part of Fig. 15.

The two-dimensional distribution of atmospheric heat budget components over the globe reflects the influence of ocean currents, orography and surface albedo in particular. It is not yet satisfactorily determined for the southern hemisphere. Likewise the vertical distribution of non-radiative heat sources and sinks is at present inadequately known even in the annual mean.

4.6 Maintenance of the atmospheric circulation

The preceding discussion with Figs. 12 and 15 has shown how cross-latitude transports of heat in the atmosphere must be invoked to explain its observed annual mean thermal structure. This implies mass transport and the existence of a circulation and hence a certain store of Kinetic energy. If the atmosphere were frictionless the circulation could persist forever and its Kinetic energy would remain undepleted. Since there is friction, work is being performed and the circulation would soon run down if new Kinetic energy were not being continuously generated. The only external energy source for the system is the sun and so there emerges a picture of the atmosphere as a *heat engine* driven ultimately by solar radiation and with a mechanical power output equal to the rate at which the Kinetic energy of the atmosphere is dissipated by friction. The ratio of the latter to the incident solar radiation provides a measure of the efficiency of the atmospheric heat engine.

Granted the analogy let us now examine the internal functioning of the atmospheric heat engine via the schematic representation of Fig. 16. It is convenient to consider three energy reservoirs, one terrestrial and two in the atmosphere. The latter are the Kinetic energy of the circulation and the so-called total potential energy of the atmosphere (the sum of thermal internal energy and gravitational potential energy- a convenient device since, in a hydrostatic atmosphere, they are proportional in the ratio c_v/R). Closer examination of the total potential energy (TPE) reservoir reveals it to be the sum of available (APE) and unavailable (UPE) total potential energy. APE is that amount of TPE which can be converted directly to kinetic energy by an adiabatic redistribution of the mass of the atmosphere to a horizontal, statically stable density stratification, a configuration achieved by the process of warm air ascent and cold air descent. The resulting atmosphere has no horizontal temperature or pressure gradients and is therefore energetically inactive with respect to the atmosphere's kinetic energy. Quite clearly then, APE is the sole energy source for the winds and the maintenance of the atmospheric circulation relies on the continuous generation of APE a process which involves heating the warmer regions and cooling the colder regions at the same elevation and so generating horizontal pressure gradients. To see what part the solar radiation plays in maintaining the atmospheric circulation we must therefore see what direct or indirect role it has in the generation of available potential energy.

The various forms of interaction between the incident solar beam and the environment are schematised on the left side of Fig. 16 with numbers (in watts metre^{-2}) indicating their magnitudes where these are known. Two are important in the present context: the heat flux of 165 watts metre^{-2} to the underlying surface and the 75 watts metre^{-2} directly absorbed in the atmosphere. Present estimates based on studies of vertical and horizontal distribution of solar absorption heating in relation to the temperature field suggest that little more than 1% of the absorbed energy goes to the available potential energy whilst the remainder simply adds to the unavailable potential energy of the atmosphere.

Consider now the fate of the 165 watts metre^{-2} heat flow to the underlying surface. Global energy balance requires a compensating upward heat flow to which three physical processes contribute; longwave radiation which

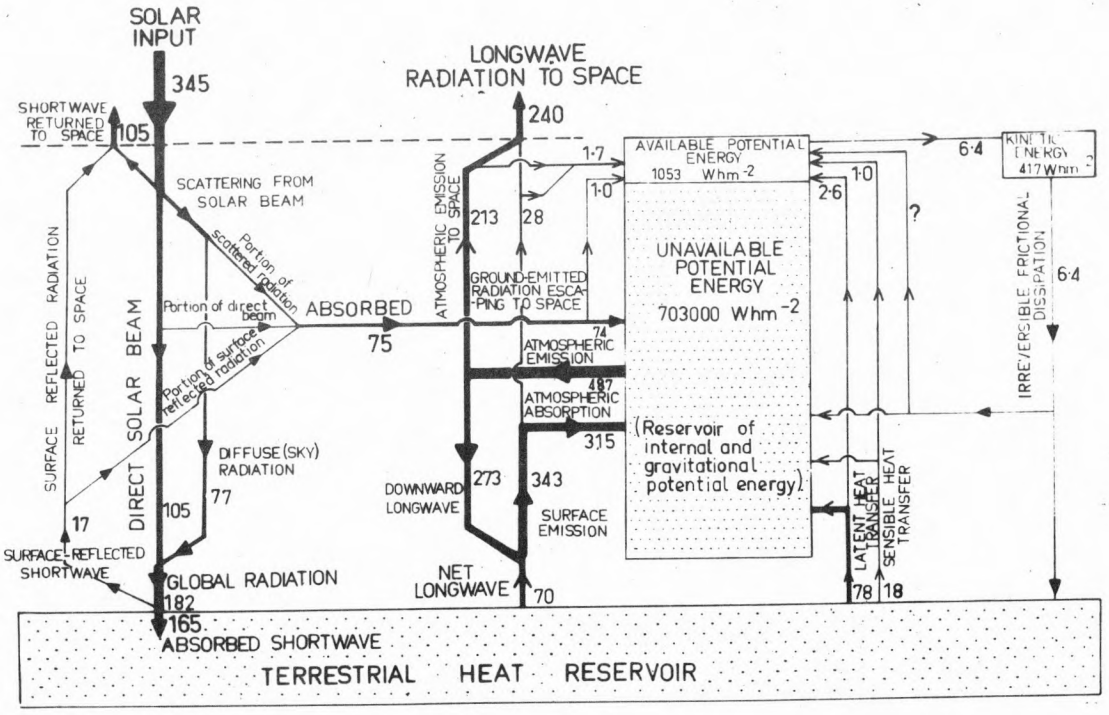

Figure 16. The global mean energy cycle of the atmosphere. Energy fluxes are in watts metre $^{-2}$ and energy contents in watt hours metre $^{-2}$. Solid arrows represent one–way energy flow and open arrows the direction in which energy flows in the global and annual mean but which may be subject to local or temporal reversal: compiled principally from the data of Vinnikov (1965), Sellers (1965), Rasool and Prabhakara (1966), Dutton and Johnson (1967) and Raschke (1968).

accounts for 70 watts metre^{-2}, contributes about 1.7 watts metre^{-2} to the available potential energy and dissipates the remainder plus another 138 watts metre^{-2} from the atmospheric reservoir to space (the details are schematised in the centre-left of Fig. 16); and latent and sensible heat flux which partition in an approximately 25 to 1 ratio between maintaining the overall temperature level of the atmosphere and generating available potential energy.

A recent estimate of frictional dissipation for the global atmosphere is 6.4 watts metre^{-2} and this is expended in heating the atmosphere and the surface with perhaps a small fraction adding also to the available potential energy. On this estimate the atmospheric heat engine has a mechanical power output of 6.4 watts metre^{-2} and an efficiency of slightly less than two percent.

We have examined only the global mean energy cycle. For a particular portion of the atmosphere the problem is complicated by the flow of mass as well as energy across its boundaries. Of special interest is the lower stratosphere which appears to act as a heat pump rather than a heat engine. Diabatic processes there produce a net destruction of available potential energy; kinetic energy imported from above or below serves as a *source* for available potential energy. Newell (1966) suggests a model in which the global atmospheric heat engine is broken down into a layered structure of heat engines and heat pumps from the surface to around 80 km with the heat engines essentially driving the adjacent heat pumps.

REFERENCES

Berland, T.G.	1960	Methods for climatological computations of global radiation. Met. Hydrol. No. 6.
	1962	Geographical principles of the solar radiation regime. Proc. All-Union Sci. Met. Conf. 1961 IV
Braginskaya, L.L., Rusin, N.P. and Strokina, L.A.	1966	Solar radiation: in Atlas of Antarctica I, Moscow.

Budyko, M.I., (ed)	1963	Atlas of the heat balance of the globe. Moscow.
Chandrasekhar, S.	1950	Radiative transfer. Oxford.
Dutton, J.A., and Johnson, D.R.	1967	The theory of available potential energy and a variational approach to atmospheric energetics; in Advances in Geophysics 12. Academic Press.
Elsasser, W.M.	1960	Atmospheric radiation tables. Meteorological Monographs 4, 12. Amer. Met. Soc.
Emden, R.	1913	Strahlungsgleichgewicht und atmosphärische Strahlung. Sitz. K. Bayer. Akad Wissensch., München.
Goody, R.M.	1964	Atmospheric radiation I. Theoretical basis. Oxford.
Halley, E.	1686	An historical account of the trade-winds and monsoons observable in the seas between and near the tropicks with an attempt to assign the physical cause of said winds. Phil. Trans. 26., 153-168.
Howard, J.N., Garing, J.S. and Walker, R.G.	1965	Transmission and detection of infrared radiation. Chapter 10 of Handbook of Geophysics and Space Environments. McGraw-Hill.
Kubota, I.	1967	On the asymetric annual variation of the temperature and solar radiation in the tropics. Geophys. Mag. 33, 4. pp. 281-386.
Lamb, H.H.	1966	The changing climate. Methuen.
Manabe, S. and Möller, F.	1961	On the radiative equilibrium and heat balance of the atmosphere. Mon. Weath. Rev. 89, 12. pp. 503-532.

Manabe, S. and Strickler, R.F.	1964	Thermal equilibrium of the atmosphere with a convective adjustment. J. Atmos. Sci., 21, pp. 361-385.
Raschke, E.	1968	The radiation balance of the earth-atmosphere system from radiation measurements of the Nimbus II meteorological satellite. N.A.S.A. Technical Note D-4589.
Rasool, S.I. and Prabhakara, C.	1966	Heat budget of the southern hemisphere: in Problems of Atmospheric Circulation (Garcia and Molone eds). Macmillan.
Schüepp, W.	1966	Direct and scattered radiation reaching the earth, as influenced by atmospheric, geographic and astronomical factors, in Robinson (ed), Solar Radiation, Elsevier.
Sellers, W.D.	1965	Physical Climatology. University of Chicago Press.
Vinnikov, K.Y.	1965	A new calculation of the heat balance of the earth-atmosphere system. Met. Hydrol. 8.
Wolfe, H.C.	1962	Symbols, units and nomenclature in physics. Phys. Today 15, 6, pp. 19-30.
Yamomoto, G. and Onishi, G.	1952	J. Met. 9, p. 415.
Yamomoto, G.	1962	Direct absorption of solar radiation by atmospheric water vapour, carbon dioxide and molecular oxygen. J. Atmos. Sci. 19, pp. 182-188.
Zillman, J.W.	1967	The surface radiation balance in high southern latitudes. WMO Tech. Note. No. 87.

APPENDIX I - SYMBOLS AND NOMENCLATURE

A. *Radiation quantities*

$I_\nu (P,\underline{r},t)$: specific intensity of a radiation field at point P in direction $\underline{r}$ and at time t: the amount of radiant energy transported in the direction $\underline{r}$ through unit area centred on P and normal to $\underline{r}$ per unit time, per unit frequancy interval and per unit solid angle.

$S_\nu (P,\underline{r},t)$: solar beam spectral irradiance at point P in direction $\underline{r}$ and at time t: the amount of radiant energy flowing through unit area centred on P and normal to $\underline{r}$ per unit time and frequency interval.

I,S : integral (i.e. wavelength integrated) intensity and solar beam irradiance.

S_E : extra terrestrial integral solar beam irradiance.

S_{VE} : the vertical component of S_E.

S_G : global radiation: the total (diffuse and direct) solar radiant energy incident on unit horizontal surface area per unit time.

S_{Go} : global radiation with cloudless sky.

D : diffuse shortwave radiant energy incident on unit horizontal surface area per unit time.

B. *Properties of a medium*

$k_{\nu iJ}$: the mass extinction coefficient at frequency ν due to process i and medium J.

ρ_J : density of medium J.

c_p : specific heat of air at constant pressure.

c_v : specific heat of air at constant volume.

R : gas constant for dry air.

N : number of scattering particles per unit volume.

n_λ : refractive index at wavelength λ.

C. *Atmospheric parameters*

$Q_{\nu iJ}$: atmospheric beam transmissivity at frequency ν after depletion by process i associated with medium J.

$q_{\nu iJ}$: zenith beam transmissivity corresponding to $Q_{\nu iJ}$

$U_{\nu iJ}$: optical path $\left(\int k_{\nu iJ} \rho_J dr\right)$ associated with depletion of a *beam* by process i and medium J at frequency ν.

$u_{\nu iJ}$: optical depth (= zenith optical path).

W_J : path integrated mass $(\int \rho_J \, dr)$ of medium J traversed by a beam.

w_{J_z} : mass of medium J above level z.

m : "absolute" air mass $\left(= \frac{p}{1000} m_r\right)$

D. *Miscellaneous quantities*

r : sun earth distance

r_e : radius of the earth

H : hour angle/height of a homogeneous atmosphere

f : Cabannes "correction" factor

σ : Stefan Boltzman constant (5.67×10^{-8} watts metre^{-2} deg K^{-4})

E. *Units conversion*

1 cal cm^{-2} min^{-1}	=	697.8 watts $metre^{-2}$
1 cal cm^{-2} day^{-1}	=	0.4846 watts $metre^{-2}$
1 Kilo cal cm^{-2} $month^{-1}$ (30.4 days)	=	15.94 watts $metre^{-2}$
1 Kilo cal. cm^{-2} $year^{-1}$	=	1.3276 watts $metre^{-2}$
1 Mw hr cm^{-2} day^{-1}	=	0.4167 watts $metre^{-2}$

APPENDIX II

BIBLIOGRAPHY

For many years there was no comprehensive treatment of radiation in the atmosphere available in the English language. Three recent publications fill this need.

(1) Goody, R.M. 1964 Atmospheric radiation I, Theoretical basis. 436 pp. Oxford.

(2) Robinson, N (ed). 1966 Solar radiation. 346 pp. Elsevier.

(3) Kondrat'yev, K. Ya. 1969 Radiation in the atmosphere. International Geophysics series, 12, 912 pp. Academic Press.

The first is a thorough, largely deductive treatment of the theory of radiative transfer in the earth's atmosphere and spectral absorption and scattering by atmospheric constituents. The second with contributions by a number of prominent workers in the field provides a readable but somewhat uneven treatment of the solar radiation, its depletion by the atmosphere, its spectral composition, methods of estimation and instruments for measurement, radiation climatology and the application of solar energy. It contains many errors and misprints. The third is an encyclopedic compilation of information on both solar and terrestrial radiation including that derived from satellite-borne sensors in the past few years. It is based heavily on the author's several earlier monographs in Russian but newer results are integrated where applicable. Several errors in the original works remain uncorrected. A great deal of the earlier Russian work unfamiliar to western workers in the field is made available for the first time.

Other important general treatments of atmospheric radiation are:

(4) Linke, F., and Möller, F. (ed). 1942-61 Atmospharische Strahlungsforschung. Handbuch der Geophysik VIII, Physik der Atmosphäre I. 1069 pp. Gebruder Borntraeger, Berlin.

the earlier chapters of which are now out of date.

(5)	Möller, F.	1957	Strahlung in der unteren Atmosphäre: in Encyclopedia of Physics XLVIII (S.Flugge, ed) Springer-Verlag. Berlin.

which presents a concise summary of the important aspects of solar and terrestrial radiation. It is however in German.

(6)	Perrin de Brichambaut, Ch.	1963	Rayonnement solaire et échanges radiatifs naturels. 299 pp. Gauthier-Villars. Paris.

and up-to-date and clearly presented but rather elementary treatment in French. It contains a wealth of numerical data.

Important additional information sources on specialised topics include:

A. *Radiative transfer*

(7)	Chandrasekhar, S.	1950	Radiative transfer. Oxford. (reprinted 1960, by Dover publications. 393 pp).
(8)	Bushbridge, I.W.	1960	The mathematics of radiation transfer. Cambridge tracts in mathematics and mathematical physics No. 50. 143 pp. C.U.P.
(9)	Sparrow, E.M., and Cess, R.D.	1966	Radiation heat transfer. 322 pp. Brooks-Cole Publishing Company, California.
(10)	Hottel, H.C., and Sarofim, A.F.	1967	Radiative transfer. 516 pp. McGraw-Hill.

B. *The sun's radiation*

(11) Zirin, H.	1966	The solar atmosphere. 501 pp. Blaisdell Publishing Co.
(12) Valley, S.L., (ed)	1965	Handbook of geophysics and space environments. Chapters 15-17, McGraw-Hill.

C. *Scattering*

(13) van de Hulst, H.C.	1957	Light scattering by small particles. 470 pp. John Wiley & Sons, New York.

D. *Longwave exchange computations for the atmosphere*

(14) Elsasser, W.M.	1960	Atmospheric radiation Tables. Meteorological monographs. 4, 12, 43 pp.
(15) Kuhn, W.R., and London, J.	1969	Infrared radiative cooling in the middle atmosphere (30-110 km) J. Atmos. Sci. 26, 2, pp. 189-204.

E. *Radiation and heat balance of earth and atmosphere*

(16) Budyko, M.I.	1956	The heat balance of the earth's surface. Leningrad.
(17) Budyko, M.I. and Kondratiev, K.Y.	1964	The heat balance of the earth: in Research in Geophysics, 2. M.I.T. Press.

(18) Albrecht, F. 1961 Der jahrliche Gang der Komponenten des Warme-und Wasserhaushaltes der Ozean. Ber. Deutschen. Wetterdienstes, 79.

F. *General circulation and atmospheric energetics*

(19) Lorenz, E.N. 1967 The nature and theory of the general circulation of the atmosphere. WMO.